The College of Engineering
University of Wisconsin-Madison

GEOLOGY OF MARE TRANQUILLITATIS AND ITS SIGNIFICANCE FOR THE MINING OF HELIUM

WCSAR-TR-AR3-9006-1

Technical Report

Wisconsin Center for
Space Automation and Robotics

●

A NASA supported Center for
the Commercial Development of Space

GEOLOGY OF MARE TRANQUILLITATIS AND ITS SIGNIFICANCE FOR THE MINING OF HELIUM

Eugene N. Cameron

Wisconsin Center for Space Automation and Robotics
University of Wisconsin-Madison
1357 Johnson Drive
Madison, WI 53706

June 1990

TABLE OF CONTENTS

ABSTRACT

Present information indicates that Mare Tranquillitatis, about 300,000 km^2 in area, is the most promising lunar source of ^3He for fueling fusion power plants on Earth. About 60% of the regolith of the mare consists of particles 100 μm or less in diameter. Helium and other gases derived from the solar wind are concentrated in the fine size fractions. Studies of very small craters indicate that the average depth of regolith exceeds 3 m in areas away from larger craters and other mare features not amenable to mining. There is no evidence of decrease of helium content of regolith with depth.

Helium is known to be enriched in regoliths that are high in TiO_2 content. Remote sensing indicates that about 90% of Mare Tranquillitatis is covered by regolith ranging from about 6% to +7.5% TiO_2; inferred He contents range from 20 to at least 45 wppm total helium (7-18 wppm ^3He).

Detailed studies and measurements of craters and inferred ejecta halos as displayed on high-resolution photographs of the Apollo 11 and Ranger VIII areas suggest that as much as 50% of the mare regolith may be physically minable, on average, with appropriate mining equipment and operations. Assuming that the average thickness of regolith is 3 m, and that 50% of the mare area is minable, the ^3He content of minable regolith containing 20 to 45 wppm total He is estimated at about 9,400 tonnes.

An area of 85,000 km^2 in the northeastern part of the mare appears to be physically more amenable to mining than the western part of the mare. It is largely covered by regolith high in TiO_2 and presumably high in He content.

Verification of the helium potential of Mare Tranquillitatis should have a high priority in the next missions to the Moon.

INTRODUCTION

Preliminary examination of possible sites for mining helium from the Moon (Cameron, 1988) focussed attention on certain maria regoliths that are high in both titanium and helium, as shown by analysis of samples obtained by the Apollo 11 and 17 missions. Mare Tranquillitatis was selected as a first target of exploration, because actual samples of the regolith are available from the Apollo 11 mission and because remote sensing indicates that large portions of the mare, comprising the western and northern parts, are underlain by high-Ti regolith. The mare is therefore a potential source of a very large amount of helium.

In my preliminary report, it was recognized that portions of the regolith in the promising areas would not be minable owing to the presence of large craters and halos of coarse, blocky ejecta around them. For a first estimate of ^{3}He potentially available, it was assumed that 30% of the total area of the mare would be minable. However, an estimate based on full and detailed consideration of the known features of the mare is obviously needed. It is also desirable to determine, so far as possible, the size and shape of minable units within the mare, since this will set constraints on the system or systems devised for mining and processing the regolith.

The present study has a five-fold purpose: (1) to delineate potentially minable areas in Tranquillitatis, (2) to examine features of the mare that will determine the ease or difficulty of mining and place constraints on mining methods and equipment, (3) to identify deficiencies and sources of uncertainty in present information, (4) to make a first estimate of tonnage of ^{3}He available from Tranquillitatis, and (5) to make specific recommendations of measures needed to remove uncertainties and to permit a final evaluation of potential mining sites and a final estimate of the amount of ^{3}He potentially available from them.

SOURCES OF INFORMATION

The following are the principal sources of information utilized in preparing this report:

A. U.S. Geological Survey, Geologic Atlas of the Moon. A series of photogeologic maps.

1) Carr, M.H., 1966, Mare Serenitatis quadrangle. Map I-489 (LAC 42), scale 1:1, 1,000,000.

2) Morris, E.C., and D.E. Wilhelms, 1967, Julius Caesar quadrangle. Map I-510 (LAC 60), scale 1:1,000,000.

3) Wilhelms, D.E., 1972, Taruntius quadrangle. Map I-722 (LAC 61), scale 1:1,000,000.

4) Scott, D.H., and H.A. Pohn, 1972, Macrobius quadrangle. Map I-789 (LAC 43), scale 1:1,000,000.

5) Milton, D.J., 1968, Theophilus quadrangle. Map I-546 (LAC 78), scale 1:1,000,000.

6) Elston, D.P., 1972, Colombo quadrangle. Map I-714 (LAC 79), scale 1:1,000,000.

7) Grolier, M.J., 1970, Sabine D region. Map I-618 [ORB II-6 (100)], scale 1:100,000.

8) Grolier, M.J., 1970, Apollo Landing Site II (Apollo 11). Map I-619 [ORB II-6 (25)], scale 1:25,000.

B. Lunar Orbiter II medium-resolution photographs 76M to 91M and 67M-74M; high-resolution photographs 76H to 91H and 67H to 74H.

C. Shoemaker, E.M., et al., 1969, Chap. 3 of Apollo 11 Preliminary Science Report. NASA Report SP-214, pp. 41-83.

D. Shoemaker, E.M., 1967, Chap. 3, Surveyor V mission report. JPL, Tech. Report 32-1246.

E. Wilhelms, D.E., 1987, Geologic History of the Moon. U.S. Geol. Survey, Prof. Paper 1348, Washington, D.C., 302 pp.

References to other sources of information are given at appropriate places in the text.

MARE TRANQUILLITATIS

General Description

Mare Tranquillitatis occupies a large basin, irregular in outline, formed by a major impact during Pre-Nectarian time (Fig. 2). In Upper Imbrian time the basin was flooded by successive flows of basaltic lava, probably accompanied by late falls of pyroelastic glass. The mare (Fig. 1) is completely covered by maps 1) to 6) of the above list. Most of the mare lies in the Julius Caesar and Taruntius quadrangles. In photogeologic mapping three major units have been recognized in the mare. From oldest to youngest, these are designated Ipm1, Ipm2, and Ipm3 or Im-1, Im-2, and Im-3. There is a confusion as to the distribution of the three units. Wilhelms (1987, p. 235) states that "Mare Tranquillitatis contains northern and southern belts of the intermediate-age group (i.e., Im-2) of Upper Imbrian basalt, separated by a belt of the young age group (i.e., Im-3)." This description does not match the distribution of the two units as shown on the maps of the Julius Caesar and Taruntius quadrangles. No belt of Im-3 is shown on the Julius Caesar quadrangle. No belts appear on the Taruntius quadrangle. There is further confusion in that neither quadrangle map matches the distribution of spectral units shown on Wilhelm's Plate 4A (Fig. 3a) or the distribution of age groups of basalts shown on Plate 9A (Fig. 3B). Unit Im-1 is found largely, but not entirely, along the margins of the mare. On the Julius Caesar quadrangle (Morris and De Grolier, 1967), which covers most of the western part of the mare, Im-2 is shown as the most widespread unit, but on the Taruntius quadrangle (Wilhelms, 1972), which covers much of the northeastern part of the mare, the most widespread unit is Im-3. Unfortunately, along the common border of the two quadrangles, the boundaries between the two units do not match. The mismatch evidently reflects differences in interpretation of unit boundaries. Finally, Plates 4A and 9A do not completely reflect variations in color shown in the color difference photograph of E.A. Whitaker (Fig. 4).

The differences between distribution of units shown on Plates 4A and 9A and distribution as shown on photogeologic maps is probably due to the fact that the maps were prepared before data

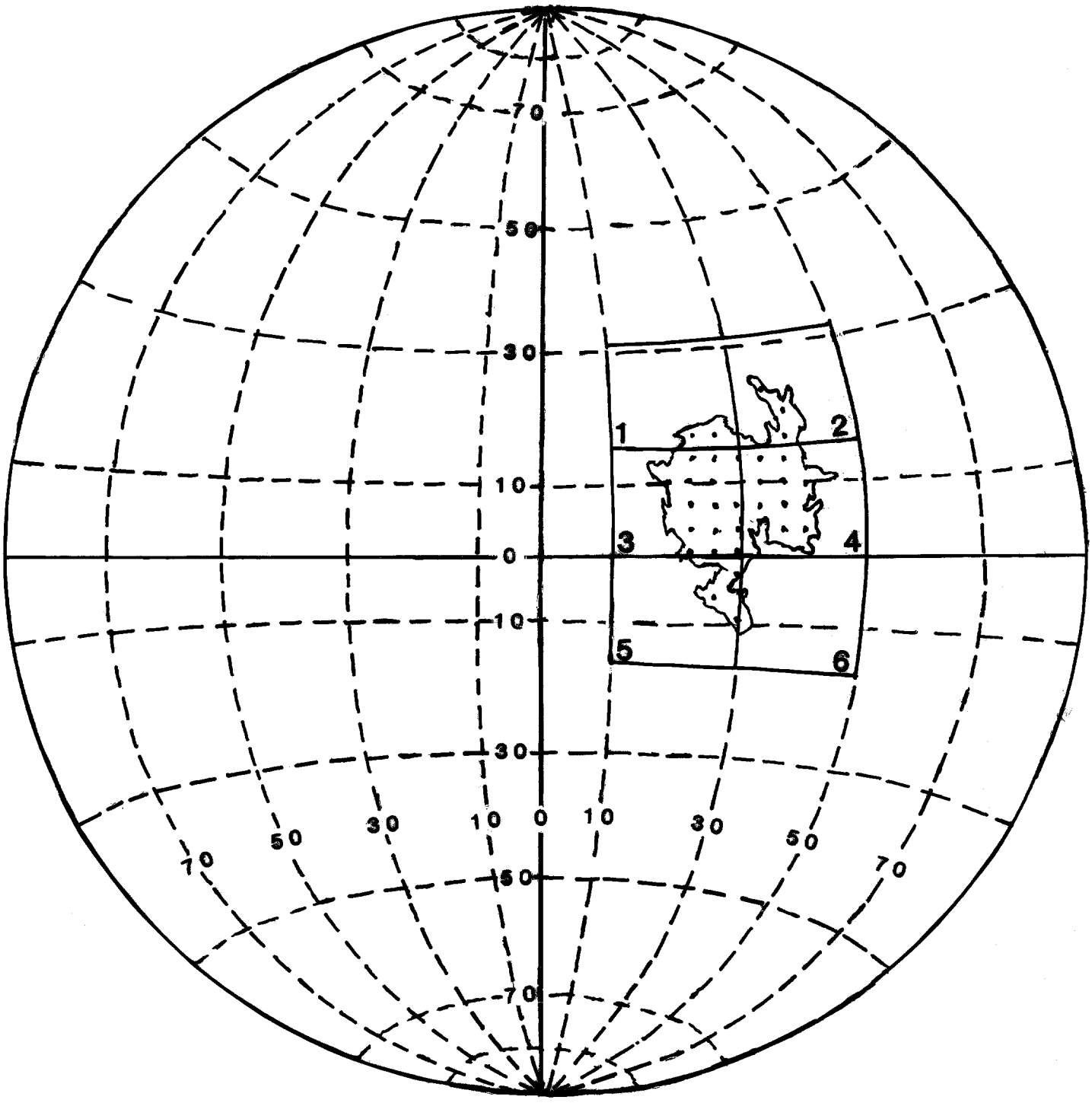

Fig. 1. Index map of the near side of the Moon, showing coverage of Mare Tranquillitatis (stippled area) by quadrangle geologic maps. 1 - Mare Serenitatis; 2 - Macrobius; 3 - Julius Caesar; 4 - Taruntius; 5 - Theophilus; 6 - Colombo.

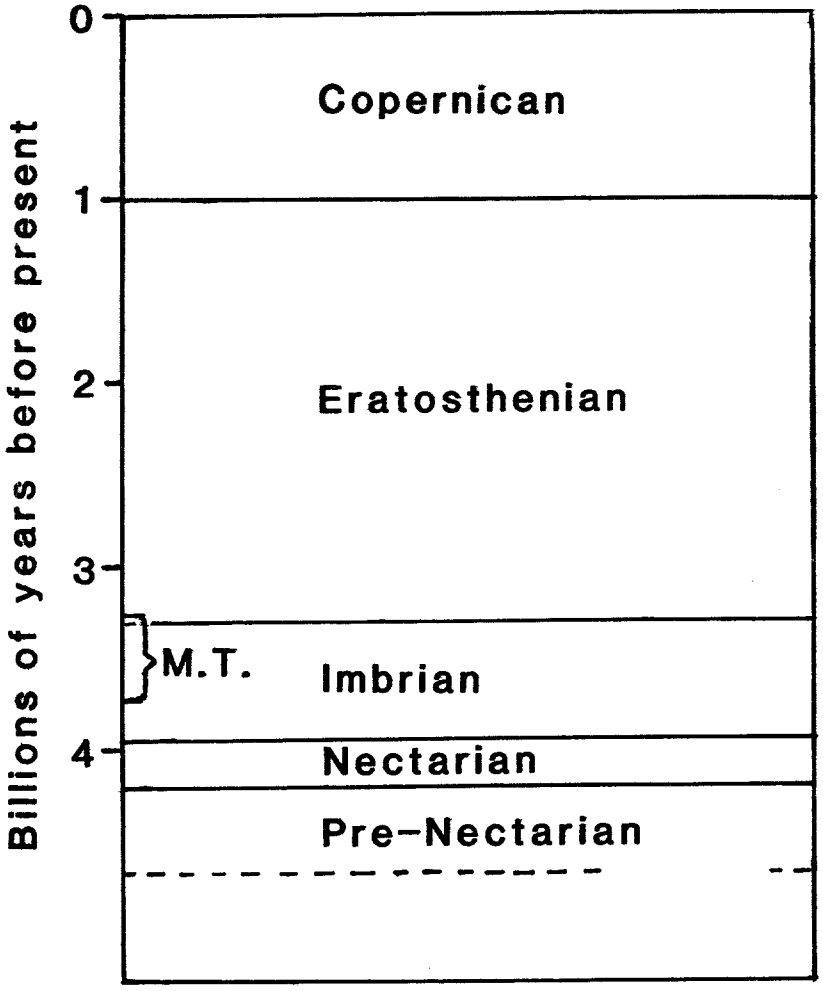

Fig. 2. Lunar time scale.

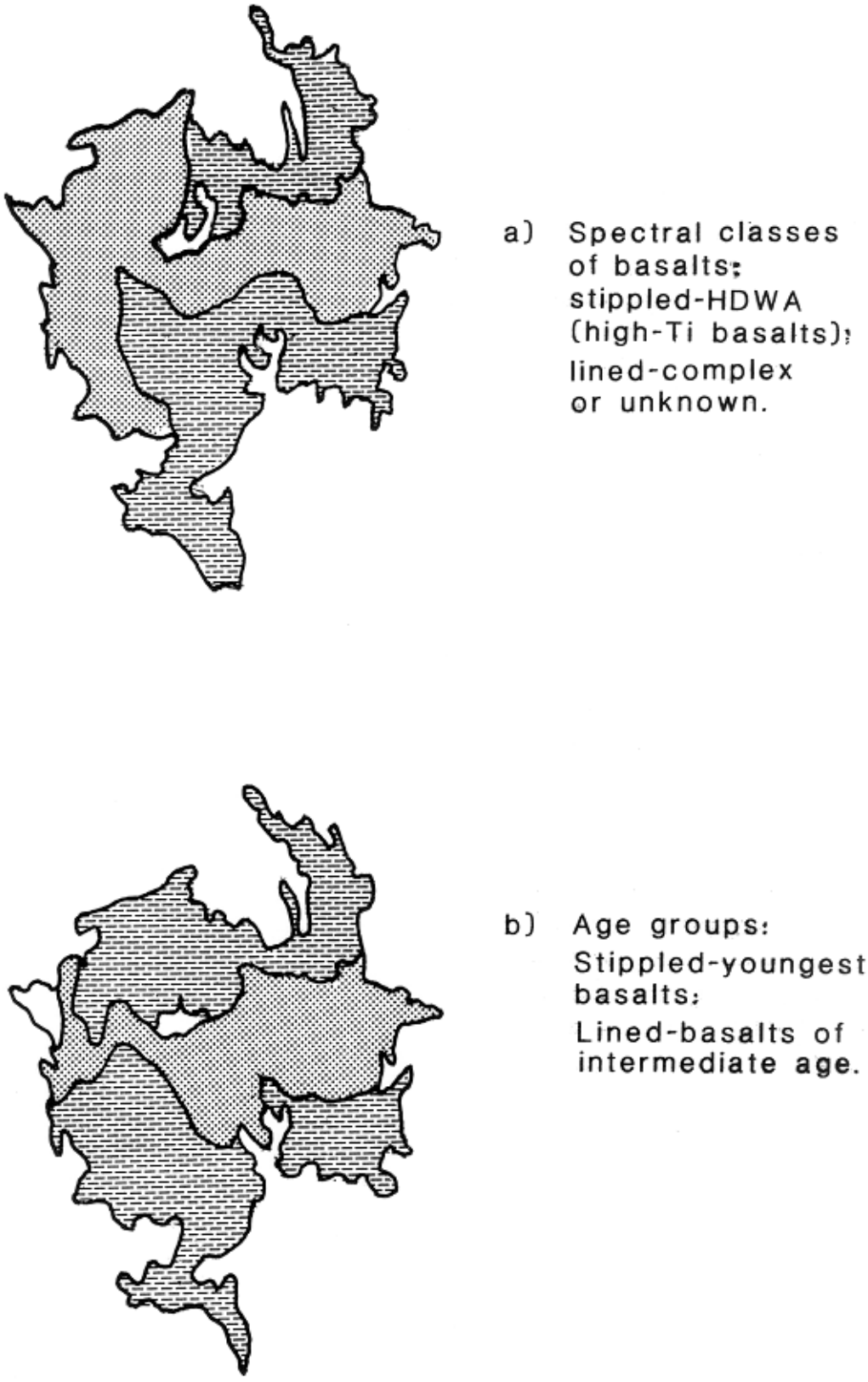

Fig. 3. Basalts in Mare Tranquillitatis, based on Wilhelms (1987), plates 4A and 9A.

Fig. 4. Color difference photograph of the near side of the Moon, made by subtracting a photograph taken at 0.31 μm from one taken at 0.61 μm. Courtesy of E.A. Whitaker.

from remote sensing become available. Those data obviously were used in preparing Plates 4A and 9A.

According to Morris and Wilhelms (1967), both Apollo 11 and Surveyor V landed on Im-2, whereas according to Grolier (1970a, 1970b), both landed on Im-1. No explanation of this discrepancy is at hand.

Pre-Mare Features

The floor of the basin over which the mare materials were erupted was highly irregular. The margins of the mare, therefore, are also irregular. The basalt flows were not thick, and in places islands of the floor rocks appear in the mare (Figs. 5 and 6). They are strikingly developed along the north and east sides of Tranquillitatis. Furthermore, certain ridges mapped on the mare appear to be related to irregularities in the floor. The most conspicuous example is Lamont (Fig. 5), a ringlike ridge that is 70 km in maximum diameter and lies NNW of the Apollo landing site. This has been interpreted as a ridge formed by settling of mare material over the rim of a large pre-mare crater. There are similar, less well developed features elsewhere on the mare. There are also pre-mare craters that are only partly buried by mare material.

Mare Features

General Statement

Much of the surface of Tranquillitatis is apparently a gently undulating surface, but there are a number of features that disturb the surface and must be considered in selecting mining sites. The most important are ridges, rilles, basement islands, domes, craters and ejecta blankets around the craters.

Ridges

Ridges 2 to 10 km in width and a few km to more than 100 km in length are a common feature of Tranquillitatis, especially in the western and northwestern parts. They range from straight to arcuate to sinuous. The characteristics of mare ridges have been summarized by Wilhelms (1987, pp. 107-110) from studies by numerous investigators. A central spine is a common feature, superposed on the rounded arch-like profile of the typical ridge. A ridge may be

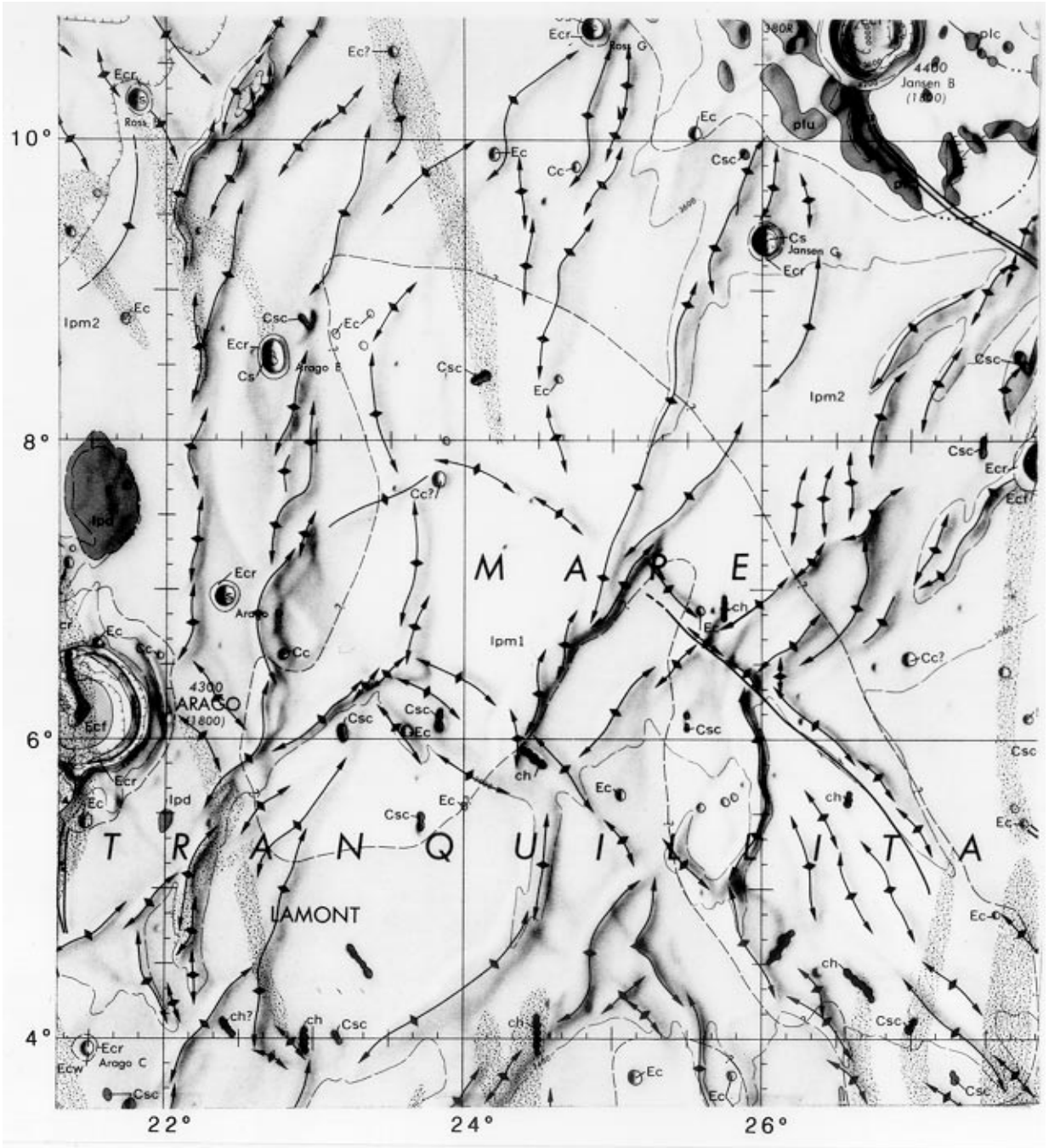

Crater materials
Copernican – Cs, Cc, Csc
Eratosthenian – Ec, Ecf, Ecr
Chain craters – Ch

Mare basaltic volcanics
Ipm3
Ipm2
Ipm1

Mare domes – Ipd

Basement materials
Plc, Plu

Fault

Ridge

Rille

Ray materials – stippled

0 30 60 km
Scale at 8°

Figure 5.
Part of geologic map of Julius Caesar quadrangle, from Morris and Wilhelms (1967).

Fig. 5. Part of geologic map of Julius Caesar quadrangle from Morris and Wilhelms (1967).

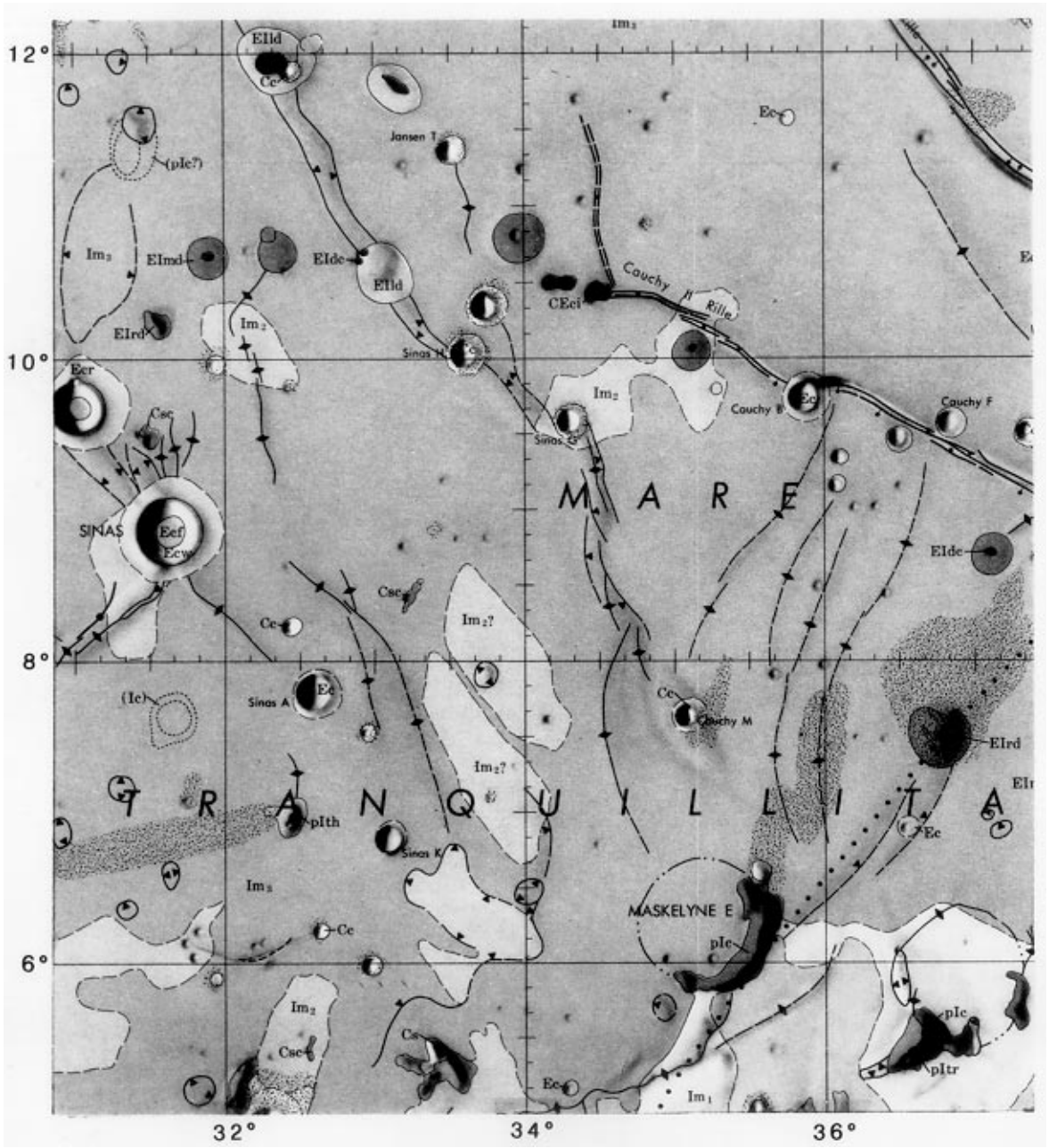

Figure 6.
Part of geologic map of Taruntius quadrangle, from Wilhelms (1972).

Fig. 6. Part of geologic map of Taruntius quadrangle from Wilhelms (1972).

bounded by a scarp or a narrow graben on one side. Ridge heights of up to 100 meters appear to be indicated.

Rilles

Rilles are graben, straight or curved, that appear to be related to subsidence along fractures. The rilles are narrow troughs with flat floors up to a few kilometers wide and steep walls 50 to 250 m high. Rilles on Tranquillitatis range from tens of kilometers to more than 300 kilometers in length. They are most numerous in the western part of Tranquillitatis, but the Couchy I and Couchy II rilles of the eastern part of the mare are respectively 275 and 210 km in length.

Domes

Domes are rounded structures, circular to elliptical in plan, that are a few to 25 km in maximum diameter. They are considered to be volcanic structures superimposed on the mare basalts. As indicated below, their total area is only a very small fraction of the area of the mare.

Basement Islands

Basement islands occur mostly close to the margins of the mare. They represent parts of the floor that were too high to be covered by the floods of mare basalt.

Craters

Craters and their ejecta blankets are undoubtedly the most important obstacle to mining on Mare Tranquillitatis. Craters are present throughout the mare. Craters visible on the geologic maps and the Orbiter II high-resolution photographs used in the present study range from 40 km in diameter (Plinius) down to 2 m, the lower limit of resolution of the photographs. Craters 5 km to 40 km are sparsely scattered over the mare; they are most numerous in the western part. Shoemaker et al. (1967) showed that the number of craters per unit area of the mare increases exponentially with decrease in diameter, and this relation has been confirmed by numerous investigators. It is apparent in any plot of diameter versus numbers of craters. Figure 7 is an example from the present study.

Impacts of bodies of a wide range of sizes have been producing craters on Tranquillitatis ever since eruption of the mare volcanics about 3.6 b. y. ago (Wilhelms, 1987). In general, the

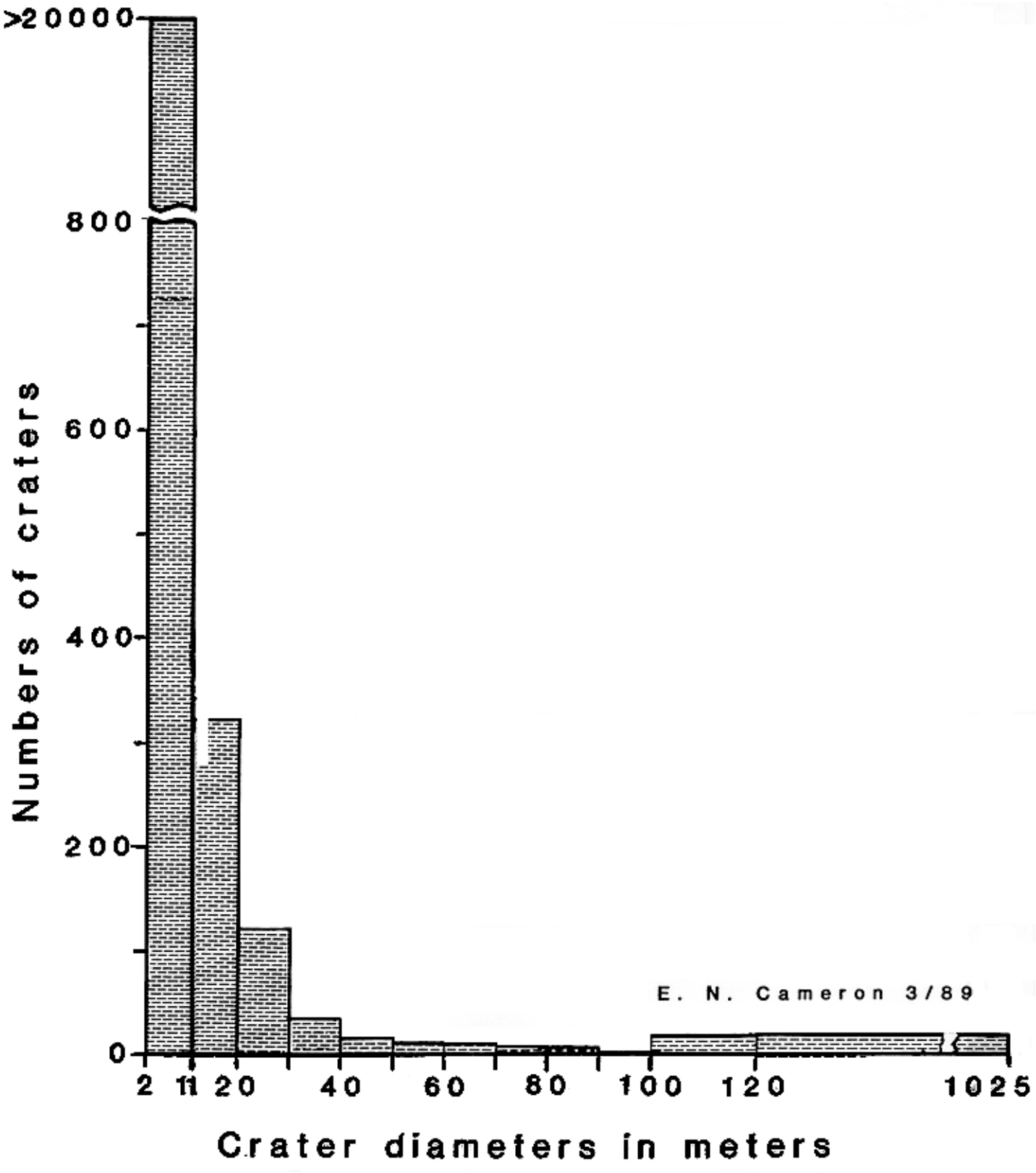

Fig. 7. Mare Tranquillitatis, Lunar Orbiter photograph II-84H_1, numbers of craters in relation to size.

characteristics of the craters are a function of their age. High-resolution photographs show a complete range from the sharp, fresh-appearing Copernican craters to older craters (very late Imbrian to Eratosthenian) that have been virtually obliterated and now appear as shallow depressions with faint rims and gently-sloping walls; they are barely recognizable as craters. Such craters show no bright halos and no blocks either inside the craters or on their rims.

The impact craters of the Moon are known to be of two genetic types, primary and secondary. Primary craters are those produced by impacts of bodies arriving on the moon from space. Secondary craters are those produced by impacts of material ejected from the primary craters. In some cases the two can be distinguished; more often they cannot. Distinction between the two types has not been attempted in the present study.

Ejecta Blankets

Ejecta blankets consist of materials thrown out of impact craters, traveling along ballistic trajectories. There is a progression from coarsest materials at or close to crater rims to finest material farthest from the rims. The halo of debris produced may be symmetrical if the meteor path is at a high angle to the surface, but the halo will become asymmetrical as the angle of incidence is decreased. Figure 8 shows an example of an ejecta halo around a Copernican crater. The white line shows the limit beyond which blocks greater than 2 m in diameter are not present. Since for each Orbiter photograph the angle of incidence of sunlight is given, depths of sharp-rimmed young newer craters can be calculated from the widths of shadows of the walls and the measured diameters of the craters. As indicated in Fig. 9, ratios for such craters vary but are mostly close to 0.25. If the diameter of a crater is more than 4 times the depth of the local regolith, blocks of bedrock are therefore likely to be found in the surrounding ejecta blanket. Around older craters, however, ejecta blocks have been partly or even totally destroyed by later impacts.

Ray Materials

Rays are elongate patterns of disturbed surface materials caused by streams of ejecta produced by impacts upon the moon. They fall into two groups. The first consists of rays that are associated with certain Copernican craters on the mare and are recognizable on photographs owing

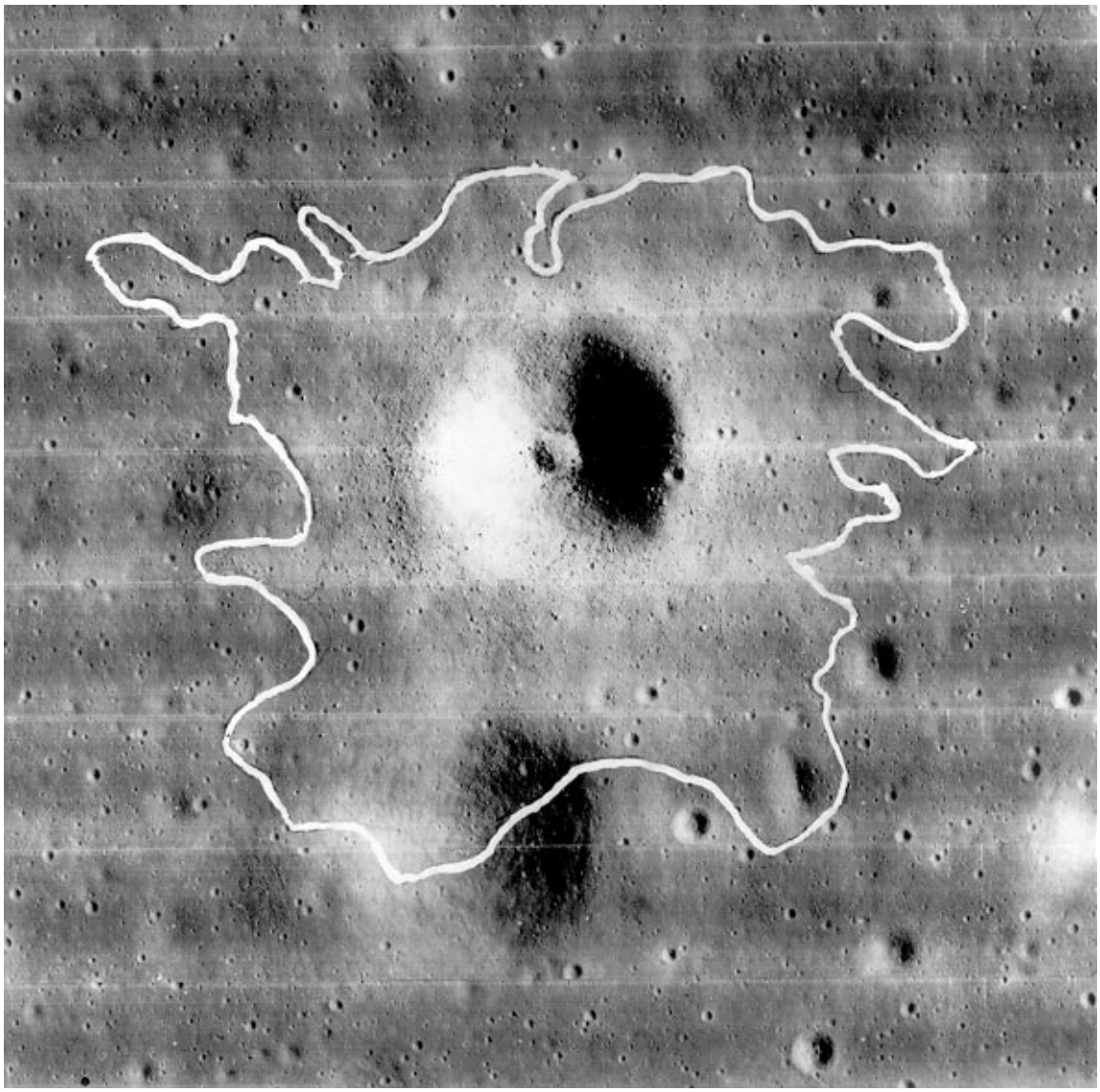

Fig.8. Copernican crater, 440 m in diameter, on Lunar Orbiter photograph II-83H_3. Ejecta blocks 2 m or more in diameter are strewn over the area bounded by the white line.

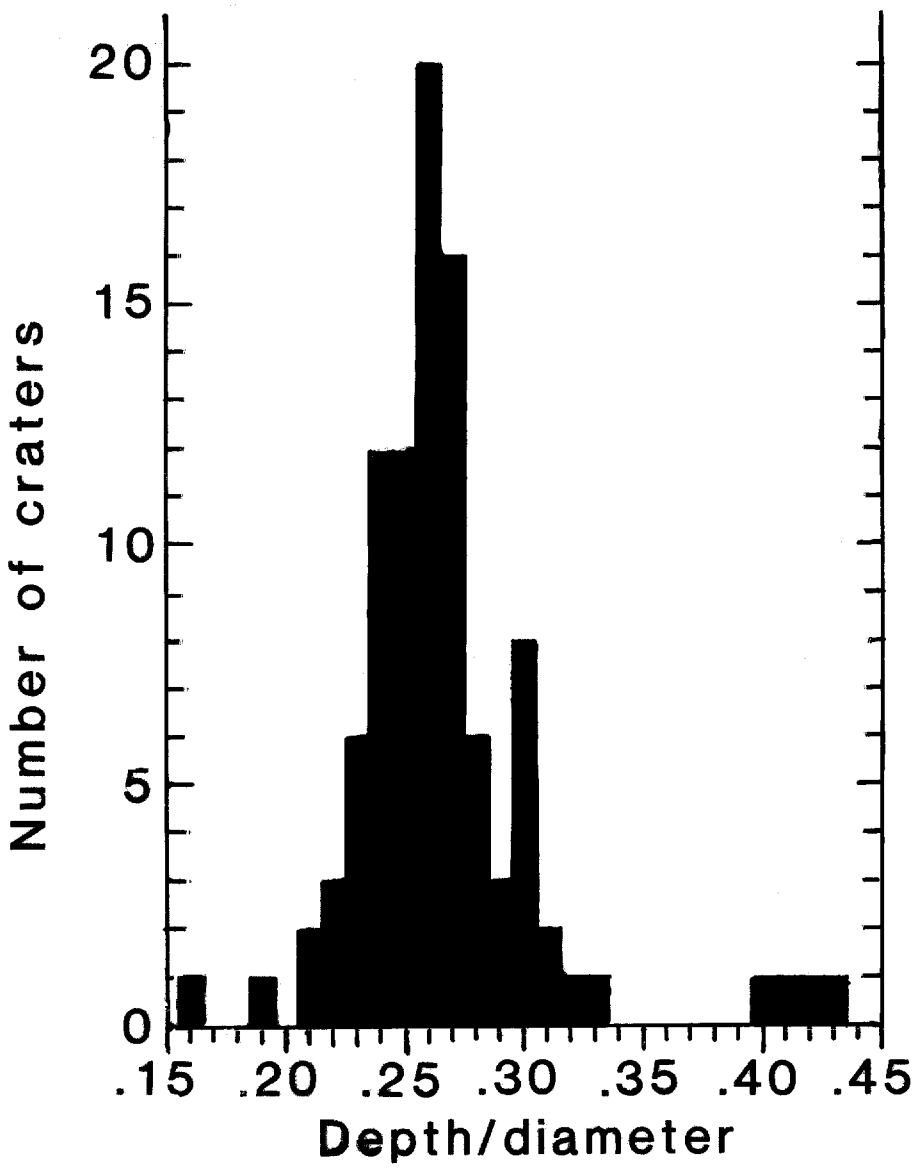

Fig. 9. Depth/diameter ratios of 98 craters, as determined from Lunar Orbiter photograph II-84H (prints H_1, H_2, H_3).

to their brightness. They extend outward 1 to 7 crater radii from the rims of craters. The second group consists of elongate to irregular areas of material; the areas range up to 85 km in length and 20 km in width. They are scattered widely over Tranquillitatis. They are considered to be disturbed regolith mixed with thin blankets of ejecta from major craters that are mostly outside the mare. Many of those on Tranquillitatis are attributed to the crater Theophilus, about 360 km south of the Apollo 11 landing site, and ray materials are most extensive in the southwestern part of Tranquillitatis, which lies directly north of Theophilus. Ray materials are poorly indicated on photographs used in the present study. The ray areas delineated on geologic maps have been plotted on the basis of telescopic observations from Earth. There appears to be little information about the composition or texture of the ray materials, other than the fact that blocks are not visible in ray materials on high-resolution photographs, so that any blocks associated with ray material must be less than 2 m diameter. Highland material is likely to be present in the rays, hence they must be considered as sources of dilution of mare-derived regolith. To what extent they will prove to be unminable, owing either to dilution or presence of blocks, is uncertain. However, the Apollo 12 landing site on a ray from the great crater Copernicus suggests that blocks will not be a significant factor.

The Mare Regolith

General Description

Lunar regoliths have been the subject of numerous studies, beginning with the pioneering work by Shoemaker and others (1967). The name is applied to the loose, predominantly fine-grained material that blankets the lunar surface. The regolith has two major components, (1) particles of minerals and rocks and (2) agglutinates. Agglutinates are mineral and rock particles welded together by glass produced by partial melting of rock and mineral material due to impacts. In the early stage of formation, a regolith consists of a high proportion of mineral and rock fragments. As gardening of the regolith by impact continues, the proportion of agglutinates rises, finally reaching a stage at which the number of particles produced by comminution is balanced by the number of agglutinate particles formed. At this point the regolith is said to be mature. In

general, the regolith of an ancient mare like Tranquillitatis will be mature. However, there will be variations in maturity where recent impacts have brought new materials to the surface.

Mare regoliths are derived mainly from the immediately underlying basaltic volcanics, but they are contaminated, perhaps everywhere, by highland material ejected from large post-mare craters in adjacent highlands and also from intra-mare craters that penetrate to the basalt layers of the floor of the mare. Thus Simon and Papike point out that whereas mare basalts from Apollo 11 and Apollo 17 contain 10.5 to 13.5% TiO_2, the overlying regoliths contain only 7.5 to 8.5% TiO_2. They attribute the difference to contamination with highland material, clearly indicated by the appearance of highland material in the modal analyses discussed below.

Modal Composition

The modal composition of the regolith at the Apollo 11 site has not been completely determined, but the composition of the 90-20 μm fraction of sample 10084 is given in Table 1, and the composition of the 1,000-90 μm fraction is given in Table 2. Lithic fragments and fused components are not included in Table 1.

Grain (particle) Size

Samples of the regolith brought back by Apollo 11 consist predominantly of particles less than 1 mm in diameter (Table 3). It should be noted, however, that no large bulk samples were obtained, and there is no information on the abundance of large blocks; such blocks would certainly not be included in the samples.

The only appraisal of particle size distribution in total regolith that I have been able to find is that of Shoemaker and Morris (1968). Those investigators made a detailed study of particle size distribution in regolith as displayed in high-resolution photographs taken at the Surveyor I, III, V, VI, and VII sites. Resolution of the photographs is 1 mm, hence only particles 1 mm and larger could be counted. Size-frequency curves were plotted for these particles and extrapolated to sizes smaller than 1 mm (Fig. 10). The curves indicate the predominance of particles less than 1 mm in diameter in the regolith. Surveyor I landed inside crater Flamsteed and Surveyor VII landed near the crater Tycho, but Surveyor III, Surveyor V, and Surveyor VI landed on typical maria,

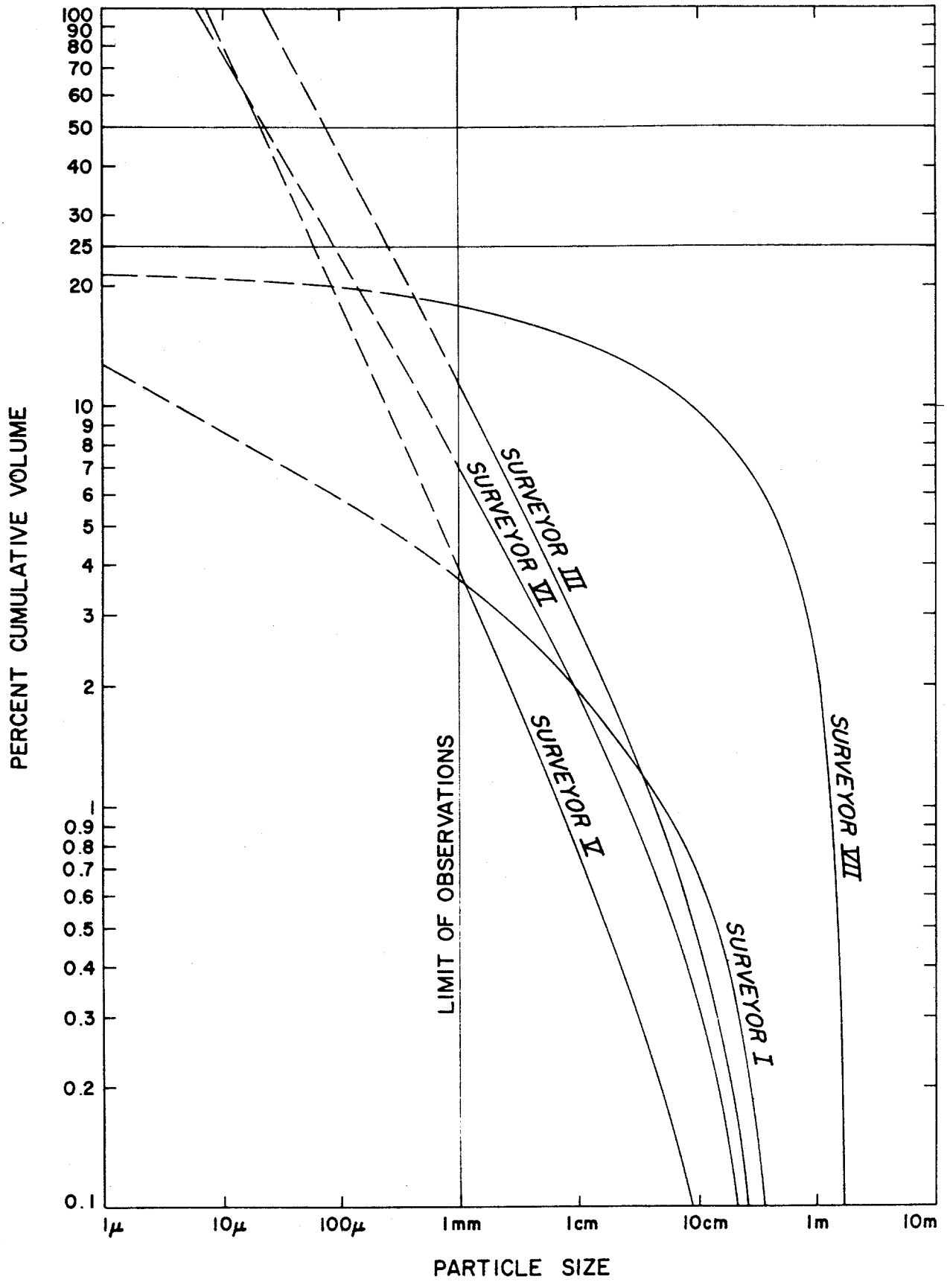

Fig. 10. Volumetric particle size-frequency distributions of particles of the lunar regolith 1 mm or more in diameter for 50% porosity. Dashed lines are extrapolations for smaller particles. From Shoemaker and Morris (1968).

Table 1

Grain Count Modal Data for the 90-20 μm Fraction of Apollo 11 Sample 10084 (Simon and Papike, 1982)

Plagioclase	21.4%
Pyroxene	44.9
Olivine	2.1
Silica	0.7
Ilmenite	6.5
Mare glass	16.0
Highland glass	8.3
TOTAL	99.9%

Table 2

Grain Count Modal Data for the 1000-90 μm Fraction of Sample 10084 (Simon and Papike, 1982)

Lithic fragments	
Mare basalt	24.0%
Highland component	2.3
Fused soil component	59.5
Mineral fragments	
Mafic	4.2
Plagioclase	1.9
Opaque	1.1
Glass fragments	4.5
Devitrified glass	1.8
Other	0.3
TOTAL	99.9%

Table 3

Grain Size Distribution in Apollo 11 Sample 10084,853 (from Criswell, 1982)

Size Fraction	Wt. %	Cumulative Wt. %
4-10 mm	1.67	1.67
2-4 mm	2.39	4.06
1-2 mm	3.20	7.26
0.5-1 mm	4.01	11.27
250 μm-0.5 mm	7.72	18.99
150-250 μm	8.23	27.22
90-150 μm	11.51	38.72
75-90 μm	4.01	42.73
45-75 μm	12.40	55.14
20-45 μm	18.02	73.15
20 μm	26.85	100.00

respectively Oceanus Procellarum, Mare Tranquillitatis, and Sinus Medii. Larger particles include both solid rock fragments derived from bedrock, and agglutinates of varying cohesion. It seems likely (H. Schmitt, personal communication) that many of the latter will be disaggregated during excavation and handling on a mining machine.

Structure

The structure of the regolith, in the few core samples brought back by the Apollo missions, has been studied in detail. A crude, mostly indistinct layering is generally present. It is inferred from this that the regolith consists predominantly of successive and interleaved thin ejecta blankets spread out around the larger craters and continually gardened by ensuing impacts.

Thickness

The thickness of the regolith on Tranquillitatis is a matter of prime importance for the mining of helium and is the controlling factor for all estimates of tonnage of regolith available. The

thickness will certainly vary from place to place. Thickness should be nil or nearly nil on the rims and floors of very young craters. Thickness should increase away from the rims. The same rules, however, should not apply to very old craters, which have undergone a long period of degradation due to gravitational slumping and continued bombardment. It seems likely that there will be very little variation in thickness of regolith across them, except for some thinning on the crater walls.

Current estimates of tonnage of regolith and design of mining machinery assume an average thickness of regolith of 3 m away from larger craters. There are no direct measurements of regolith thickness on the surface of Tranquillitatis. Estimates of thickness are based on studies of craters and ejecta as displayed on lunar photographs, mathematical modeling of the mechanics of crater formation, and passive seismic experiments. Shoemaker et al. (1967) noted at the Surveyor V landing site that two craters respectively 15 m and 20 m in diameter were surrounded by strewn fields of blocks. Assuming crater depth to diameter ratios of between 1/3 and 1/5, they concluded that the depth of regolith is not greater than 5 meters. Shoemaker et al. (1970) estimated regolith thickness at the Apollo 11 landing site at 3 to 6 m. This estimate is based on the observed depths of anomalous flat-floored craters and craters with central mounds, assuming that the floors are at the top of the bedrock surface. Nakamura et al. (1975), from the passive seismic experiment, calculated the depth of regolith at the Apollo 11 site as 4.4 m.

The writer believes that information on the thickness of the regolith over broad areas is best obtained at present from studies of very small craters on high-resolution photographs of the mare. A special study of very small craters on high-resolution photographs of the area east of the Apollo 11 landing site has therefore been made. Findings of the study are the following:

1. Almost all craters less than 12 m in diameter (the smallest visible are 2 m in diameter) are fresh craters with sharp rims. Presumably they are of Copernican age.
2. Many such craters are superimposed on older larger craters with less distinct rims.
3. The density of fresh craters, as indicated by counts of sample areas, is in the neighborhood of 1,000 per km^2.

4. Depth-diameter ratios of most small fresh craters are very close to 0.25 (Fig. 9). This holds for small craters away from larger craters as well as for those superimposed on older craters.
5. Fresh craters less than 18 m in diameter have smooth walls and floors. No blocks or other irregularities are visible within them. Bedrock was evidently not penetrated by the craters.

From these observations the following conclusions can be drawn:

1. By the time the young, fresh craters began to be formed, most older craters less than about 4.5 m deep (less than 18 m in diameter) had been obliterated by impacts.
2. By early Copernican time the regolith was already about 4.5 m deep.
3. An estimate of 3 m for the average depth of regolith away from larger craters is therefore conservative, especially in view of the presence of regolith more than 3 m deep on the rims of older craters.

In a subsequent section, the conservative estimates of an average depth of regolith of 3 m and a ratio of depth to diameter of 0.25 are used as the basis for delineating block-strewn areas around craters; i.e., areas of regolith containing blocks of bedrock.

Helium Content

Information on the helium content of the regolith of Mare Tranquillitatis is from two sources: (1) analyses of samples taken from the Apollo 11 landing site and (2) inferences based on the relationship between the He contents and the TiO_2 contents of lunar regoliths in general.

Helium contents of various Apollo 11 samples are given in Table 4. The data are for bulk samples and for "breccias", particles produced by impact-welding of regolith particles. Note that the average He content of breccias is higher than the average content of the fines, despite the fact that analyses of size fractions of fines invariably show that He is enriched in the finest fractions (Fig. 11), whereas the breccia particles are much coarser. No explanation of this anomaly is at hand.

The precise value of the samples as indices of the He content of the mare away from the landing site is in doubt. According to Wilhelms (1987, p. 235),

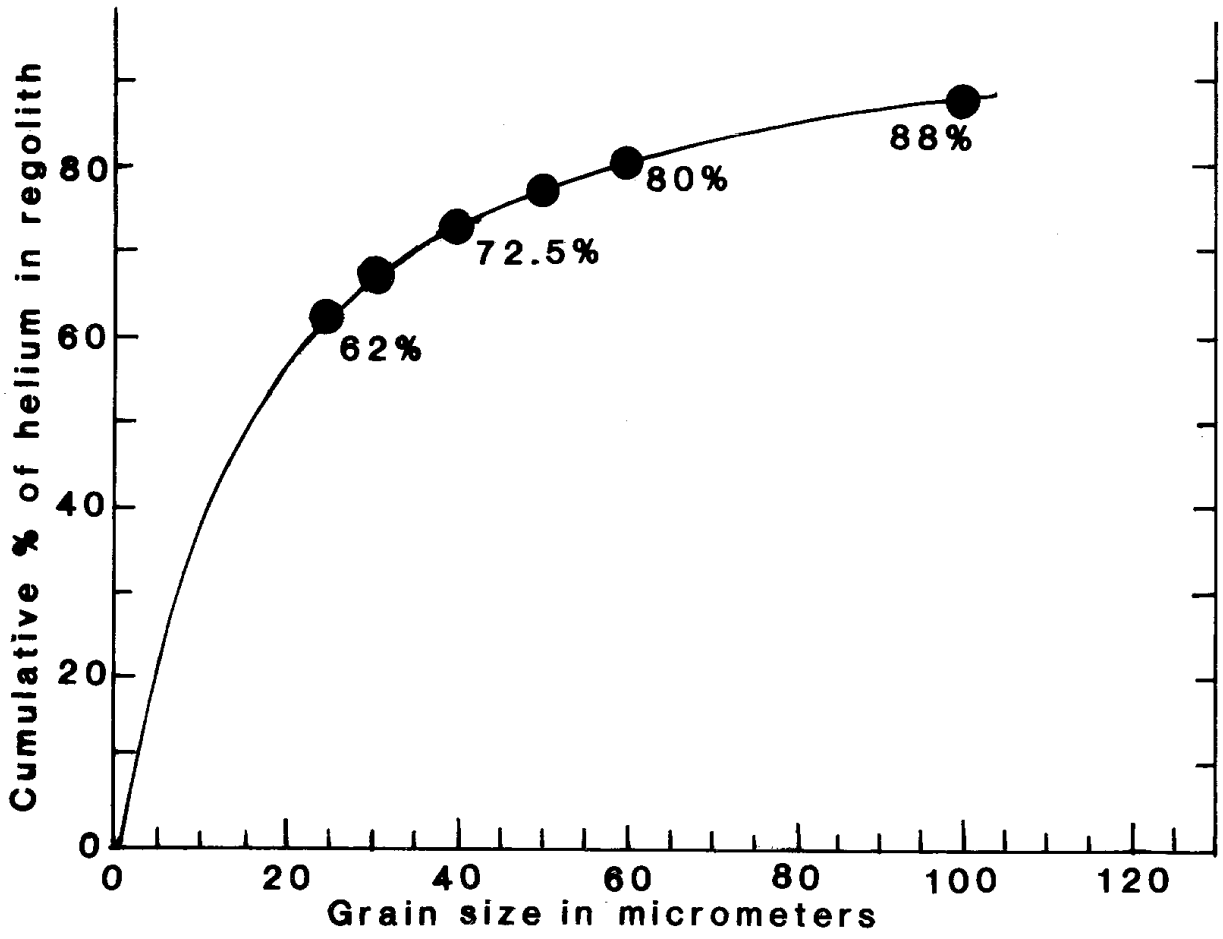

Fig. 11. Percentage of total helium in relation to grain size in Apollo 11 regolith sample 10084, based on data from Criswell and Waldron (1980) and Hintenberger et al. (1970).

Table 4

Helium-4 Contents of Apollo 11 Samples

A. Regolith Samples

Sample	He-4 wppm	Reference
10084,18, fines	34	Hintenberger et al., 1970
10084, 18, fines	37	
10084,8, fines	34	
10084,40, fines (1)	44	Funkhouser et al., 1970
10084,40, fines (2)	41	
10084,29, fines (1)	40	Marti et al., 1970
10084,48, fines (1)	35	Pepin et al., 1970
10084,48, fines (2)	40	
10084,40, fines (3)	40	

B. Breccia Samples

10021,20	67	Hintenberger et al., 1975
10046,16	36	
10048,27	56	
10060,24	58	
10061,11	58	
10061,33	60	
10018	43	Funkhouser et al., 1971
10021	67	
10023	45	
10027	27	
10048	38	
10061	85	
10068	45	

"The landing point of the lunar module Eagle was about 400 m west of the 180-m-wide, 30-m-deep crater "West" between blocky rays of that Copernican crater (... Shoemaker and others, 1969; Schmitt and others, 1970) ...Beaty and Albee (1978, pp. 431-432; 1980) suggested that almost all the samples were derived from the ejecta of the West crater and came from no more than about 30 m deep. Because most of the samples were exposed to the space environment for about 0.1 aeon (Eberhardt and others, 1970; Guggisberg and others, 1979), West is probably about 0.1 aeon (10^8 yrs) old. At least one sample (10050) has an exposure age of 0.5 aeon (5×10^8 yrs)..." and thus appears derived from another source.

It appears from this description that the Apollo 11 landing site may be on regolith that is younger than the normal regolith of the surrounding mare, has had a shorter time of exposure to the solar wind, and may be lower in helium content.

All samples of regolith returned from the Apollo 11 site are surface samples, hence there is no direct information on variation in the He content of the regolith of Mare Tranquillitatis with depth. However, samples from drill holes at the Apollo 15, Apollo 16, and Apollo 17 sites are relevant here, since they suggest what variations in He content with depth may be expected in lunar regoliths. Results of analyses of cores from drill holes at the three sites are given in Table 5. The Apollo 15 and Apollo 16 cores show variation in He content but no correlation of content with depth. The average He content of the Apollo 15 samples is 10.8 wppm. The average for 11 Apollo 15 surface samples is 11.1 wppm. The average for Apollo 16 core samples is 6.4 wppm. The average for 22 surface samples (Hintenberger and Weber, 1973; Haskin et al., 1973; Walton et al., 1973) is 6.7 wppm. The Apollo 17 drill core shows an increase in He content with depth. Apollo 17 samples are too heterogeneous to permit calculation of a meaningful average He content. At any rate, core and surface samples give no indication of a systematic decline, or increase, in the He content of regolith with depth. This is hardly surprising. Given the repeated overturn of regolith due to impact gardening during the more than 3 billion years since Mare

Table 5

Helium-4 in Apollo 15, Apollo 16, and Apollo 17 Cores

Apollo 15*

Sample	Depth cm	He-4 wppm
15001	149	15
	154	11
	160	13
	163	12
	168	12
	176	9
	187	6
	206	7
15003	217	13
	220	14
	226	9
	231	13
	238	10
	242	10
	246	9
	253	11

Apollo 16**

Sample	He-4 wppm
60007 (top barrel)	4-7
60006	5-7
60004	8-9
60003	6-8
60001 (bottom barrel)	4

Data for 5 of 7 core barrels representing depths of about 13 cm to about 200 cm.

Apollo 17[+]

Sample	Depth cm	He-4 wppm
70008,163,284		8
70008,205,228/283		9
70008,15,285		13
70006,10`		13
----------140----------		
70005,10		23
70004,10		21
70003,10		20
----------240----------		
70002,10		17
70001,10		21
----------290----------		

*Hübner et al., 1973. **Heymann et al., 1978. [+]Pepin et al., 1975.

Tranquillitatis was formed, no systematic pattern of variation with depth is likely to be found. Instead, an irregular pattern of small-scale variation, both vertically and laterally, is to be expected. For any given site, the range of helium content is likely to be that shown by surface samples.

Samples from the Apollo 11 landing site provide the only direct evidence of the He content of the regolith of Mare Tranquillitatis. The He content of the regolith of the mare as a whole must be inferred from data for lunar regoliths in general. For maria regoliths, the following findings (Cameron, 1988, 1990) are critical to the delineation of areas of regolith that are enriched in He:

(1) Regoliths of certain maria or parts of maria contain less than 20 wppm He, but regoliths of certain other maria have He contents ranging from 25 to nearly 50 wppm.

(2) The He content of a mare regolith is a function of its composition. In particular, the He content is related to its TiO_2 content (Fig. 12). Regolith enriched in TiO_2 is likewise enriched in He. The TiO_2 content of regolith, as indicated by remote sensing, can therefore be used as an index of the He content. It is so used in evaluation of potential mining areas in Mare Tranquillitatis in the following section of this report.

MINABLE AREAS IN MARE TRANQUILLITATIS

General Statement

There are three major questions to be answered in determining the minability of regolith in Mare Tranquillitatis:

(1) What percentage of the total area of the mare is covered by high-Ti regolith, and what variations in He content within high-Ti areas are to be expected?

(2) How much of the total area of the mare, roughly 300,000 km^2, is physically amenable to mining for ^3He?

(3) What are the distribution, shapes, and sizes of the minable areas?

Pending further investigation of the mare, no final answers to these questions can be given. The following sections, however, summarize available relevant information and provide preliminary answers.

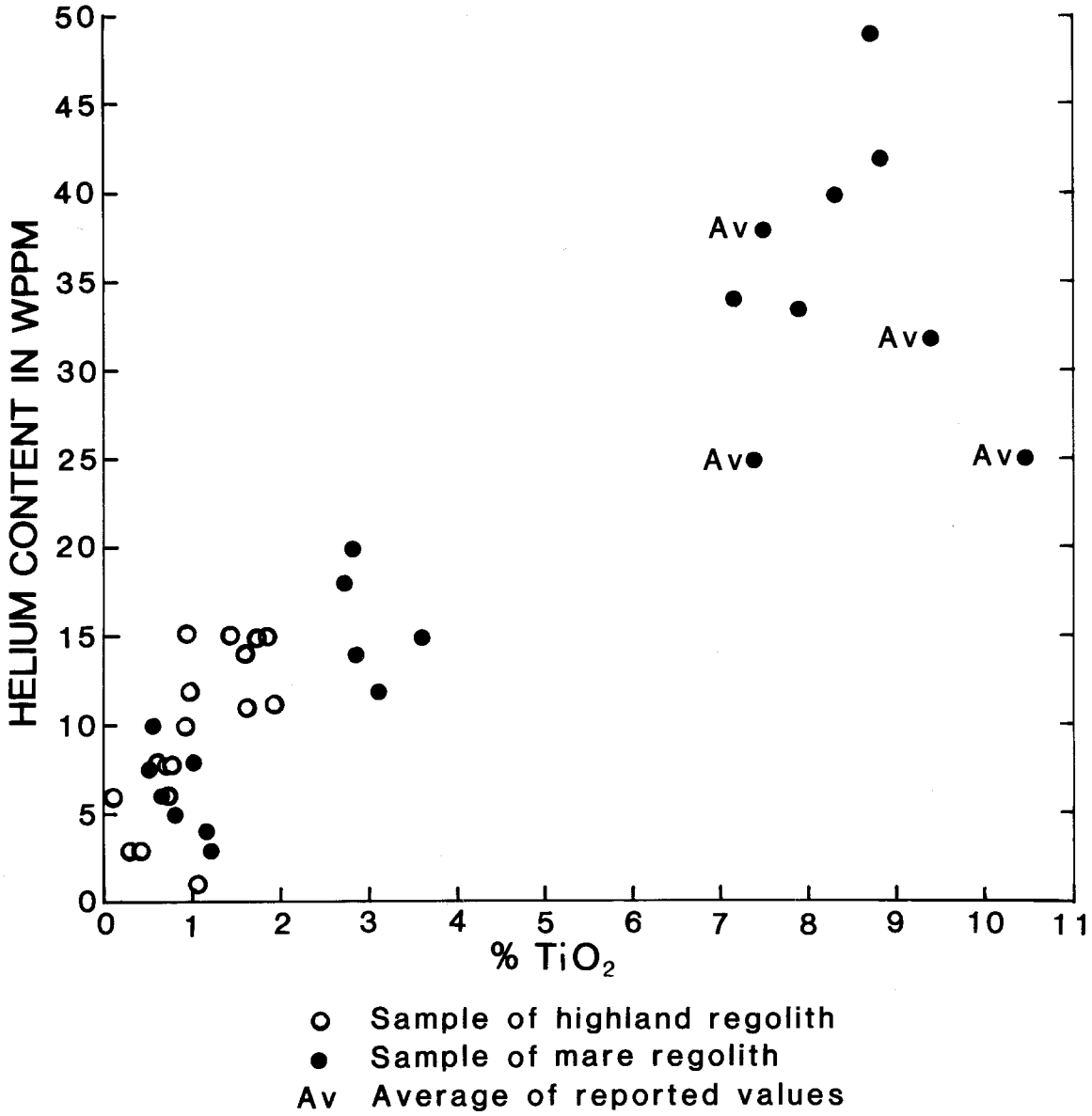

Fig. 12. Relation between He contents and TiO_2 contents of lunar regolith samples. Data from Bogard and Hirsch (1978), Bogard and Nyquist (1972), Criswell and Waldron (1982), Cuttitta et al. (1971), Cuttitta et al. (1973), Eberhardt et al. (1970), Eberhardt et al. (1972), Eugster et al. (1975), Funkhauser et al. (1970), Heymann and Yaniv (1970), Heymann et al. (1972), Heymann et al. (1973), Heymann et al. (1978), Hintenberger et al. (1970), Hintenberger et al. (1971), Hintenberger et al. (1974), Hintenberger and Weber (1973), Hubner et al. (1973), Hubner et al. (1975), Kirsten et al. (1972), Laul et al. (1974), Laul and Papike (1980), Laul and Schmitt (1973), Ma et al. (1978), Marti et al. (1970), Nava (1974), Pepin et al. (1970), Pieters et al. (1980), Pieters and McCord (1976), Rose et al. (1974), Wilhelms (1987), Willis et al. (1972).

Percentage of the Mare Occupied by High-TiO_2 Regolith

As indicated previously (Cameron, 1988), information on the distribution of high-titanium regolith in Mare Tranquillitatis, apart from the Surveyor V and Apollo 11 sites, is entirely from remote sensing. The most detailed information is from the color difference photograph by Whitaker (Fig. 4) and the spectral ratio map of Johnson et al. (Fig. 13). Figure 4 covers the entire mare, whereas Fig. 13 does not include the northeastern part. For the parts covered by both, agreement is good, if we take into account that in Fig. 13 all high-Ti regolith is lumped into a single category of +6% TiO_2. Areas in the category 3 to 6% TiO_2 correspond closely to the brightest areas in Fig. 4. However, on Fig. 4 the remainder of the mare shows as black areas interspersed with areas that are various shades of dark to medium gray. The only interpretation of the pattern possible at present is that the spectrum of grays reflects variations in the TiO_2 content of regolith within the area shown on Fig. 13 as having +6% TiO_2. If the lower limit is slightly more than 6%, then the upper limit is about 7.5%. This is the content of Apollo 11 regolith; Apollo 11 landed on a black area or on an area that is black finely mottled with dark gray.

On an enlargement of Whitaker's photograph the areas of Mare Tranquillitatis occupied respectively by black regolith, dark to medium gray regolith, and light gray regolith have been outlined and are shown in Fig. 14. Calculations from measurements indicate that 28% of the mare is covered by black regolith in part mottled with dark gray, 65% by dark gray to medium gray regolith, and 7% by light gray to white regolith. The inferred TiO_2 contents of the three classes are respectively 7.5%, 6 to 7.5%, and 3 to 6%. The black regolith should contain 30 to perhaps 45 wppm of He, the dark to medium regolith presumably will contain 20 to 30 wppm He. However, the need for verification is evident.

The estimates of helium content apply to mature regolith. Maturity is a function of length of exposure to the solar wind. Given the nature of the process of gardening of the regolith by impacts, exposure time may vary both laterally and vertically in the mare. Such variations cannot be detected by any of the available methods of remote sensing. However, the great age of Mare Tranquillitatis and the evidence that successive generations of craters have been created and then

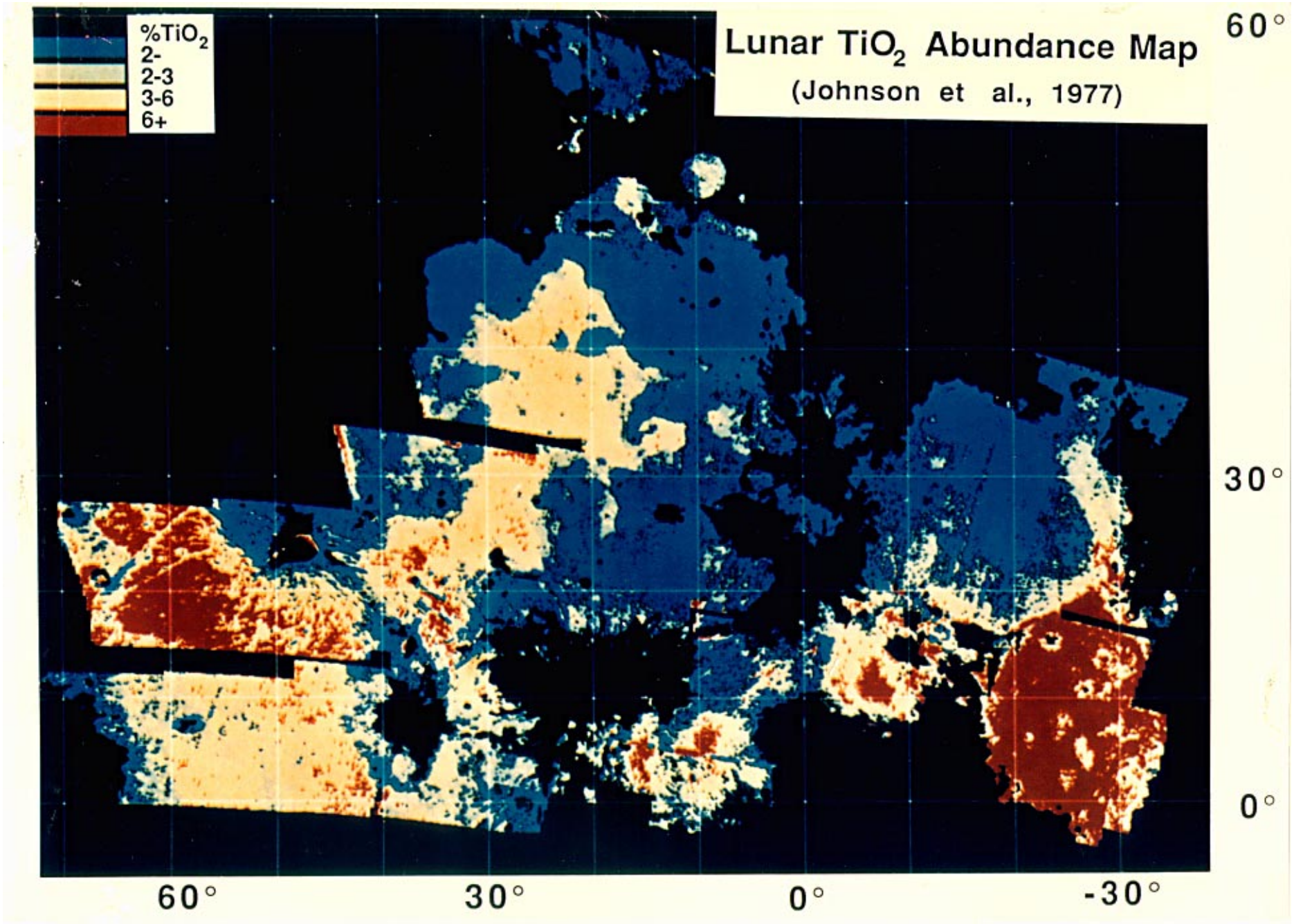

Fig. 13. Spectral ratio map of parts of the equatorial belt of the lunar near side, showing variation in TiO_2 abundance of regolith as inferred from measurements of the 0.38 μm/0.56 μm ratio. From Johnson et al. (1977).

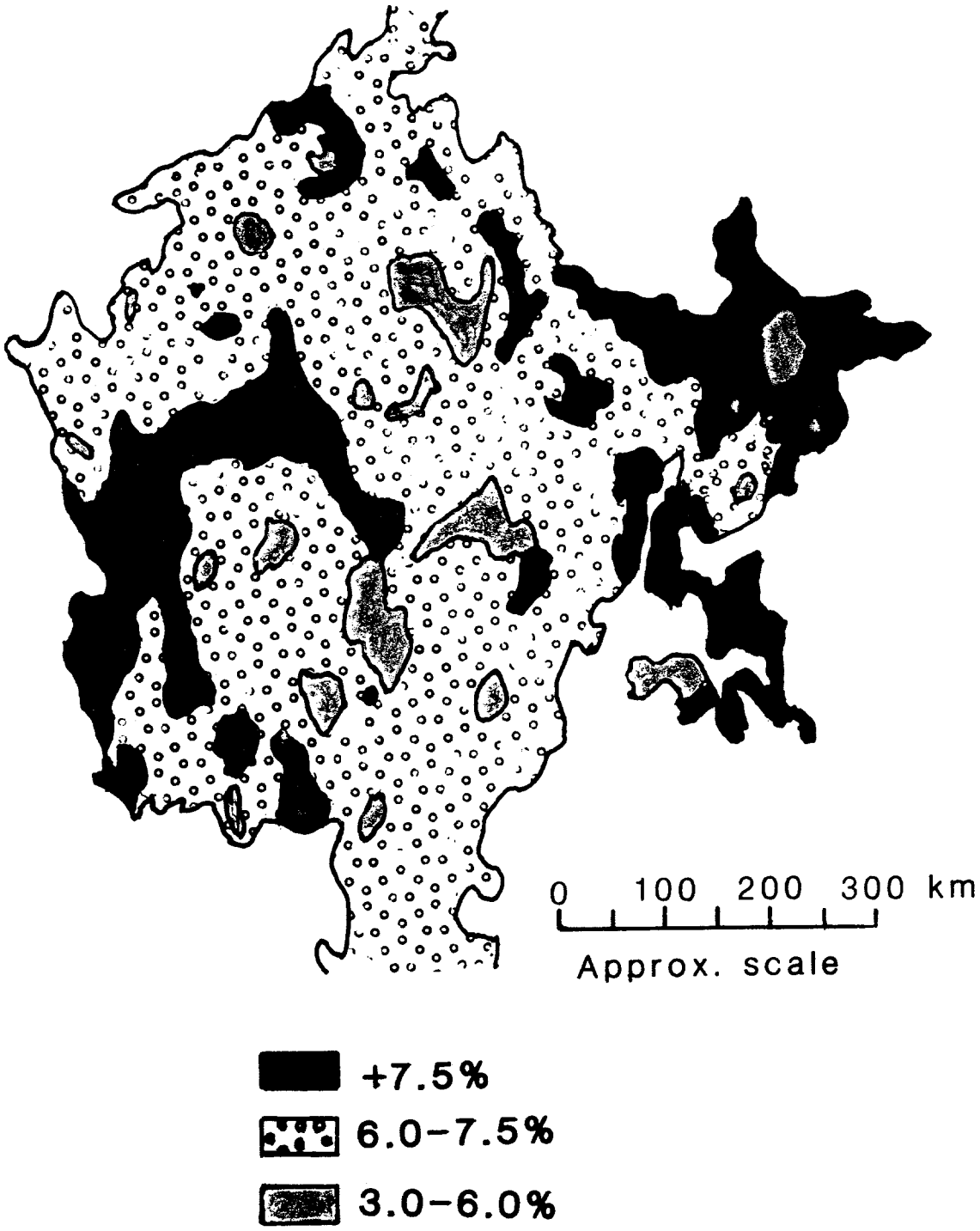

Fig. 14. Inferred variations in TiO_2 content of regolith of Mare Tranquillitatis.

destroyed or largely destroyed by impacts, it seems reasonable to infer that much of the mare is underlain by mature regolith. Besides maturity, degree of dilution with highland material will also affect the helium content. Only systematic sampling can determine actual patterns and degree of variation.

Percentage of the Mare Physically Amenable to Mining

General Remarks

Ideally, mining areas should be flat or gently undulating. Steep-walled craters will not be minable, and the total of the areas occupied by such craters must be subtracted from the total area of the mare in calculating the total minable area. The total area of ejecta halos with coarse blocks must also be subtracted; the halos may be unminable or minable only at unacceptable costs. Ridges, rilles, and domes must be subtracted, at least until there is better knowledge of their minability. For a conservative estimate, it is probably desirable to subtract the areas occupied by rays, again until better information about these features is at hand.

In terms of information presently available, the percentage of Mare Tranquillitatis that will be physically amenable to mining cannot be fully determined, but preliminary estimates can be made from information furnished by geologic maps and photographs.

Information from Geologic Maps

The chief value of the geologic maps is the information they contain as to the extent and distribution of major features that constitute unminable ground. About 87% of the Tranquillitatis lies within the Julius Caesar and Taruntius quadrangles, so that these are the principal source of information on major features of the mare as a whole. The area of the mare occupied by major features on the two quadrangles has been calculated from measurements of the intercepts of the various features on east-west lines 1 degree apart. The results indicate that approximately 24% of the mare will be unminable owing to major structures and other major features (Table 6). If the areas occupied by rays prove to be largely or entirely minable, the figure is reduced to about 18%.

Table 6

Percentages of the Total Area of Mare Tranquillitatis on the Julius Caesar and Taruntius Quadrangles Occupied by Major Features

Domes	0.6%
Ridges	5.6
Craters	4.2
Rilles	0.6
Basement materials	2.0
Miscellaneous non-mare features	3.4
Ray materials	5.6
TOTAL	22.0%

Table 6 indicates that the distribution of major features is not uniform over the mare. There is a marked disparity between western and northeastern parts of the mare. Of the area of about 85,000 km^2 in the northeastern part of the mare outlines on Fig. 15, only about 11% is occupied by major features. If rays prove to be minable, the percentage unminable due to major features is even less.

The map of the Sabine D region gives a larger-scale view of a rectangular area 62.5 by 52 km, or 3,250 km^2, in the southwestern part of Tranquillitatis. The Apollo 11 landing site lies within the map area, near the southwestern corner. Percentages of the total map area occupied by various major features (Table 7) have been calculated from measurements on 16 equally spaced lines 2.3 km apart and parallel to the long sides of the map. The greater number of major features in the southwestern part of Tranquillitatis and the large areas of ray material are reflected in the table. The extension of the mare southward into the Theophilus quadrangle, if mapped on the same scale as the Sabine D region, would probably show an even higher percentage of total area occupied by structural features and ray materials. The extension does not appear promising as a mining area.

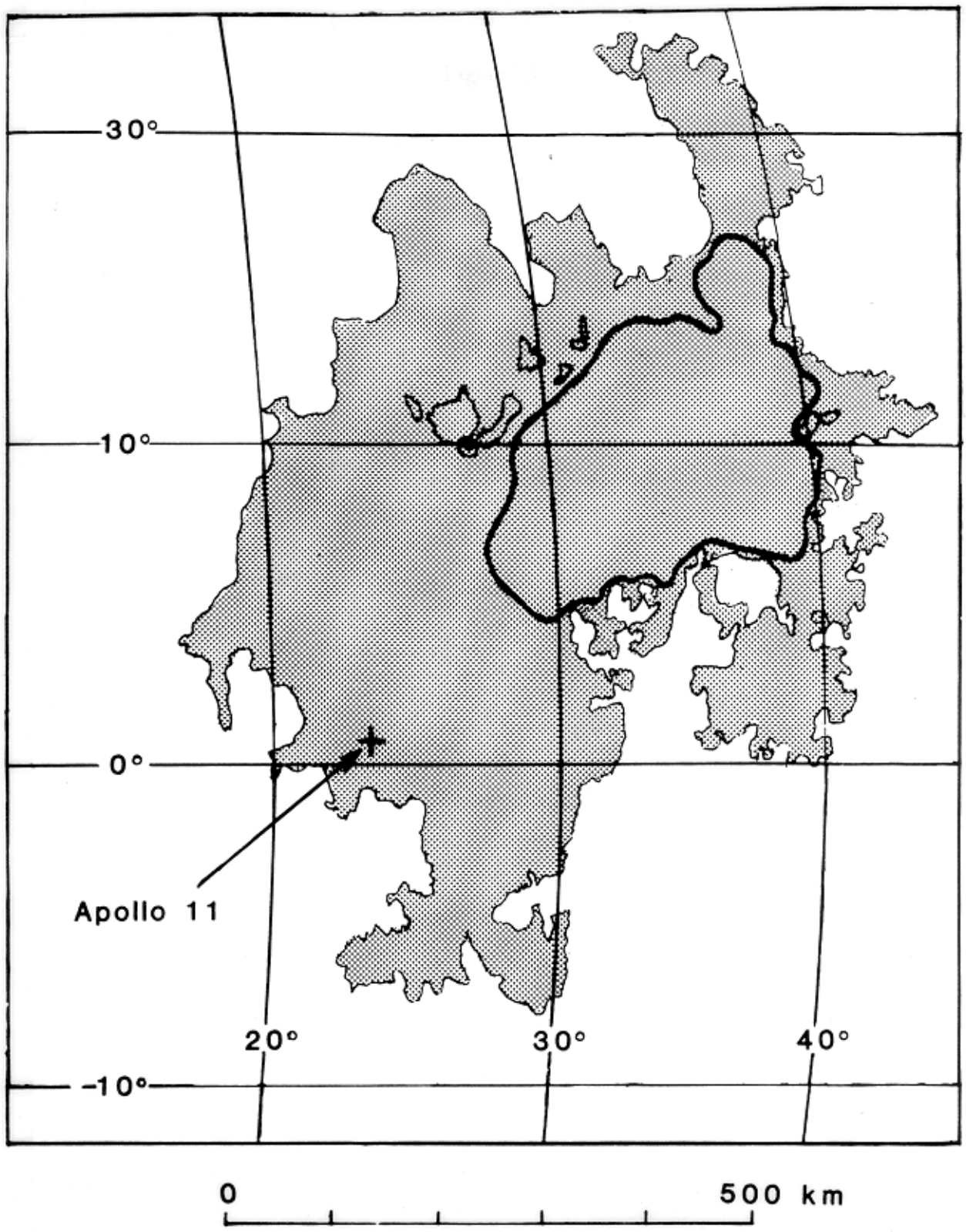

Fig. 15. Map of Mare Tranquillitatis. Major structural features are less numerous in the area bounded by the area bounded by the heavy black line than in the remainder of the mare (cf. Figs. 5 and 6).

Table 7

Percentages of the Sabine D Region Occupied by Major Structures and Other Features

Domes	<1.0%
Ridges	4.9
Craters and crater materials	16.9
Basement materials	<1.0
Ray materials	16.0
TOTAL	38.0%

Minable Areas as Determined from High-Resolution Photographs

Estimates of minable areas from geologic maps are only partial estimates. Their principal value is in indicating gross differences in minability between various major portions of Tranquillitatis. In order to approximate more closely the extent of minable areas, it is necessary to take into account craters and their ejecta blankets that are too small to be shown at the scales of the geologic maps.

As noted earlier, mining areas should be flat or gently undulating. Steep-walled craters will not be minable, and the total of the areas occupied by such craters must be subtracted from the total area of the mare in calculating the total minable area. The total of the areas occupied by ejecta halos with coarse blocks must also be subtracted; such halos may be unminable or minable only at unacceptable costs. Data for both craters and blocky halos must be obtained by measurements of these features on high-resolution photographs of portions of Tranquillitatis. Lunar Orbiter II high-resolution photographs were used for the present study. Photographs II-76H to II-91H make up two overlapping series that cover a rectangular area about 35 by 30 km. The Apollo 11 landing site lies 1 km from the west boundary of this area and 4 km north of the SW corner. The Surveyor V landing site is about 14 km west of the northwest corner of the area. Except that no

rilles or domes are present, the area has the full range of structural and other features displayed on Mare Tranquillitatis.

A second set of high-resolution photographs, II-67H to II-74H, covers an area 16.4 by 33 km that includes the Ranger VIII impact site. In general character this area resembles the area covered by the first set of photographs.

There are three problems in measurement of craters and ejecta halos. The first is the range of craters, from fresh craters with steep walls to very old craters that are so indistinct as to be almost unrecognizable. The fresh craters are obviously unminable. The very old craters cause only undulations of the surface of mature regolith. It seems likely (1) that such craters will pose no physical obstacles to mining and (2) will have regolith of sufficient depth and time of exposure to the solar wind to qualify as helium ore. However, in measuring craters, any attempt to draw a line between the two categories of craters quickly degenerates into a purely subjective exercise. I have therefore measured all craters on a given photograph, from fresh and sharp to indistinct. The result is certainly a conservative approach to estimation of unminable ground.

The second problem is that only blocks 2 m or more in diameter can be seen on the photos. Ejecta blankets outlined from the distribution of visible blocks therefore understate the extent of blocky ground. This will be especially true for ejecta halos around young craters like that shown in Fig. 8. There is no unequivocal solution of this problem. For purpose of the present study, with the advice of Harrison H. Schmitt, the following rules have been adopted:

(1) If no blocks are visible, either in or adjacent to a crater, the unminable area is taken as a circle centered on and having the diameter of the crater.

(2) If blocks are visible inside a crater, but not on the rim or outside it, the unminable area is taken as a circle centered on the crater and having a diameter twice that of the crater.

(3) If blocks are visible both on the rim and outside the rim, the unminable area is taken as a circle centered on the crater and having a diameter three times that of the crater.

The validity of these rules will be established only through future experience on the Moon, but my own studies of the high-resolution photographs persuade me that the rules will yield

reasonable approximations of areas potentially unminable owing to the presence of abundant blocks of bedrock and that the overall result will be a reasonable and conservative estimate of the percentage of Tranquillitatis that will be minable.

The third problem lies in errors of measurement. I estimate that for sharp-rimmed craters, the error is ±0.2 mm for the crater diameter. As crater rims become less distinct, the accuracy of measurement undoubtedly falls off. More than this, for reasons noted above, it is not always possible to be sure what is or is not a crater, rather than an undulation of the mare surface or an artifact of the photography.

Replicate measurements of a few photographs indicate that two successive sets of measurements will not agree either in the numbers of craters measured or in the total areas calculated from the measurements. The error indicated is about 10% of the percentage given; i.e., if the percentage of the area of a photography occupied by craters and associated blocky ground is given as 20%, the probable error is ±2.0%.

Measurement of Craters and Ejecta Halos

Each high-resolution photograph covers a strip, with long dimension oriented nearly north-south, approximately 18 km long and 4.5 km wide, divided into three end-to-end prints. From south to north these are designated H1, H2, and H3. Photos 83H, 84H, and 85H were initially selected for measurement as reasonably representative of the area east of the Apollo 11 landing site. On each of the 3 prints of a photo, measurements were made for all craters with diameters 1 mm (approximately 11.7 m in actual diameter) or greater.* The results are shown in Table 8.

The series of H-2 prints from photos 84H2 to 91H2 gives an east-west transect across the area covered by high-resolution photographs 76H to 91H. Results of measurements for the series are given in Table 9.

* To avoid misunderstanding, it should be pointed out that in general older craters (except the smallest ones) have younger craters superimposed on them. For example, a crater 200 m in diameter may have 30 or more superimposed visible craters. In Tables 8, 9, and 10, such a crater will be represented by a single measurement of the diameter of the large crater, from which the area occupied by the crater plus its ejecta halo, if any, will have been calculated. This area then becomes part of the total unminable area from which the percentage shown in the last column has been determined.

Table 8
Data from Photographs II-83H, II-84H, and II-85H

Print	No. of Craters Measured	Percentage of Area Unminable
II-83H1	1081	10.8
II-83H2	575	22.4
II-83H3	581	11.0
II-84H1	589	8.9
II-84H2	490	7.8
II-84H3	736	8.5
II-85H1	461	7.9
II-85H2	639	13.0
II-85H3	481	14.0
Average		11.5

Note: In this table and in Tables 9 and 10, "Percentage of Area Unminable" means the percentage of the area occupied by craters 1 mm (11.7 m) or more in diameter plus associated halos of blocky ground. See text for explanation of rules of measurement.

Table 9

Data from Photographs 84-H2 through 91-H2

Print	No. of Craters Measured	Craters 1 to 2 mm in Diameter	Percentage of Area Unminable
II-84H2	618	283	7.8
II-85H2*	947	560	14.1
II-86H2*	987	630	15.4
II-87H2*	775	507	11.3
II-88H2*	1129	776	12.3
II-89H2*	872	572	13.3
II-90H2*	1331	887	13.1
II-91H2*	902	622	12.8
Average			12.5

*Overlap with previous print excluded from measurement; e.g., the portion of 85H2 overlapping 84H2 is excluded, and so on.

The tables show that there is a substantial variation in percentage of area unminable from one part of the Apollo 11 area to another. For the area of any given print, the percentage is strongly affected by the number and size of the larger craters, which are erratically distributed over the mare. However, from print to print there is variation in the density of craters; this is best indicated by the data for numbers of craters having diameters from 1 to 2 mm, but there are also variations in the density of larger craters. The effect of this on minability of portions of the mare is discussed below.

Table 10 gives data for 10 high-resolution prints of the area of the Ranger VIII impact. Here again there is a considerable variation in unminable area from one print to another. Large percentages are due to large craters or areas of large craters, which are very erratically distributed over the Ranger VIII area. It is worth noting that there is no indication of this on the 1:1,000,000 map of the Julius Caesar quadrangle, and again it is clear that this map and the map of the Taruntius quadrangle have only limited value as guides to the distribution and amount of minable ground.

The successive H2 prints, 67H2 to 74H2, give an east-west transect across the midsection of the area covered by the total assemblage of prints. It is evident from the tables that the average percentage of unminable ground is higher for the Ranger VIII area than for the Apollo 11 area, but there is marked variation in the percentage in the Ranger VIII area. In part this is due to the presence of numerous large craters. They are concentrated in one belt that runs north-south through prints 71H2 (northern portion), 71H2, and 71H3, and in another belt that runs northwest-southeast through 72H3, 73H3, and 73H2. Print 71H2 is representative of the first belt. It has not only large craters but closely spaced craters of intermediate size. The whole area of the print must be considered unminable, with adjacent portions of 71H1 and 71H3. The same is true of northern 72H2 and the southern part of 72H3. On the total assemblage of prints, however, there are large areas for which the unminable percentage will range from about 12 to 15%.

Table 10

Data from Photographs II-67H to II-74H

Print	No. of Craters Measured	Percentage of Area Unminable
II-67H1	796	10.9
II-67H2	664	23.2
II-67H3	549	25.9
II-68H2	806	15.0
II-69H2	847	12.1
II-70H1	597	26.1
II-70H2	930	11.1
II-71H2	520	50.4
II-72H1	780	20.1
II-72H2	740	16.4
II-73H2	619	39.0
II-74H2	883	15.8
Average		22.2

Other Factors Affecting Minability

The minability of a portion of a mare is affected by other factors besides crater-halo area; namely, crater distribution over the area, crater size distribution, and the capability of the mining system for excavating blocky material along with the finer regolith and rejecting all coarse material so as to process only the fines. The first factor is illustrated in Fig. 17. This chart is an overlay of print II-84H3 (Fig. 16). Each circle on the chart represents a crater, with its halo of ejecta if present, the extent of the halo being determined according to the rules for measurement described above. The center of each circle is the center of the crater. The minimum thickness of regolith is assumed as 3 m outside craters and halos. The chart clearly indicates the effect of distribution on the size of intervening minable areas. The worst possible case is one in which the craters are evenly distributed. This will produce minable areas of minimum size. The best case is that of pronounced clustering of craters; minable area will then be much larger.

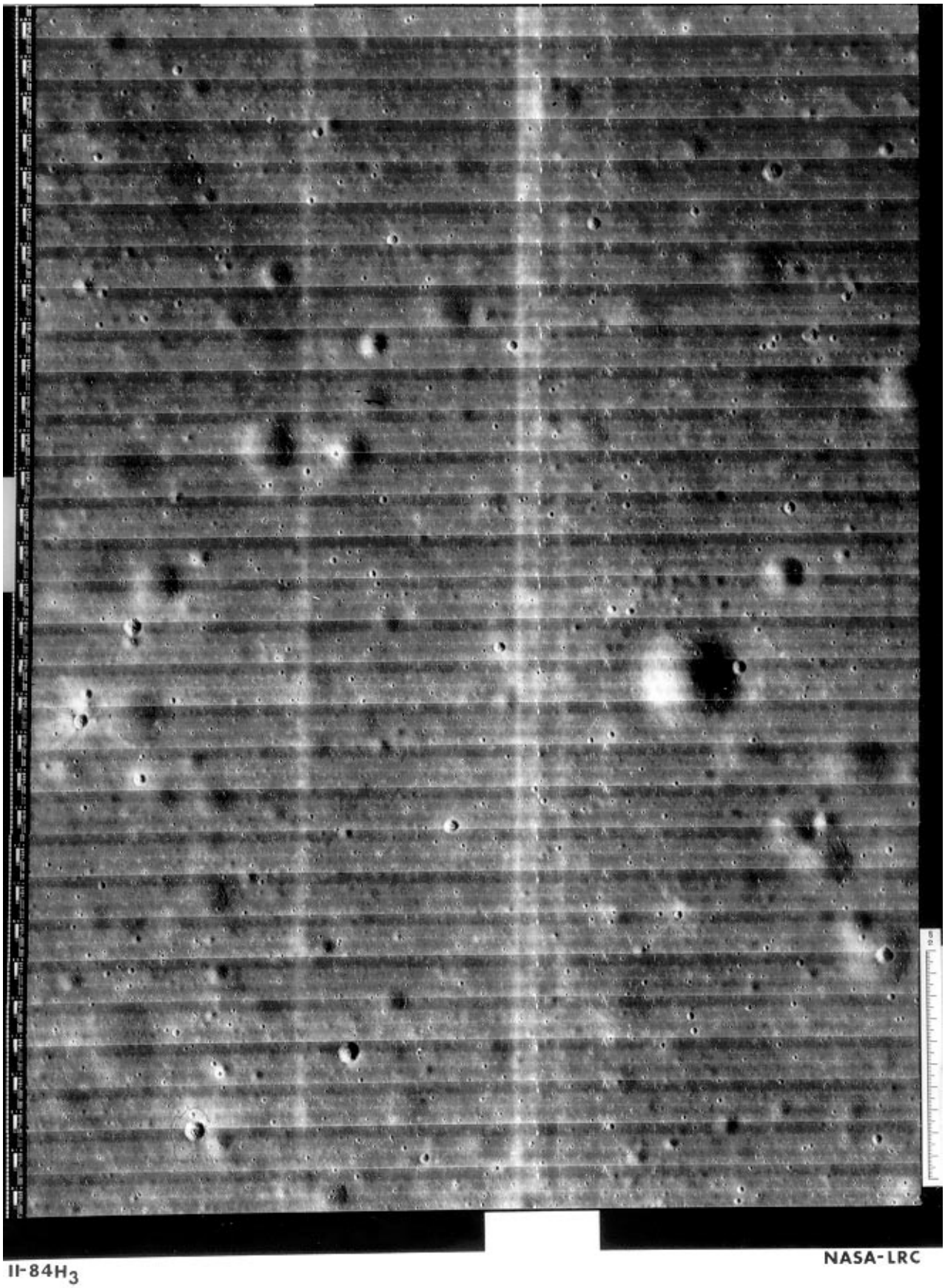

Fig. 16. Lunar Orbiter print II-84H_3. Note range in distinctness of craters. Reduced from original size of 39×53 cm.

The effect of size distribution is best considered in conjunction with the capability of the mining system for handling blocky material. The effect of the latter is clearly shown by a comparison of Figs. 17 and 18. In Fig. 17 it is assumed that the mining system cannot handle blocky material. It must therefore avoid all craters 1 mm (11.7 m) or more in diameter on the photographs since these may be accompanied by blocky halos. Suppose that the minimum area for an efficient mining unit is 400 m by 400 m. The figure shows that the number of mining areas available is very limited. If, however, the mining system is capable of sorting out blocks from the regolith and discarding them, craters up to 2.0 mm (23.4 m) in diameter on the photographs can be mined. The number and size of mining areas available is greatly increased. For the case illustrated in Fig. 17, the percentage of the total area minable would not exceed 15%. In the case of Fig. 18 the minable area of 400 m square blocks plus contiguous extensions (shaded) would exceed 40%. The significance of the size distribution of craters now becomes apparent. The total number of craters in an area may be large, but if there is a significant fraction in the 1.0 to 2.0 mm (11.7 to 23.4 m) range, a substantial percentage of the total area may still be minable with a scheme of square mine blocks.

Assuming an average minable regolith thickness of 3 m and a regolith density of 2.0, the total minable regolith in unit blocks and sideward extensions in the area of Fig. 18 is 71,400,000 tonnes. At the mining rate of 4,960,000 tonnes per year estimated for the machine designed by Sviatoslavsky and Jacobs (1988), the area would supply the machine for 14.4 years.

Pending analysis of the cost effectiveness of mining in relation to the design and operation of mining machines and the size and shape of mining units required for efficient operation, the selection of a 400-meter square mining unit is arbitrary, though it may prove to be not unrealistic. If it proves economically feasible to mine smaller units or to mine around and between craters, the minable percentage of the total area will be increased. In Fig. 19 the basic mining unit is taken as 300 meters square, but no blocks can be handled, hence craters 11.7 m or more in diameter must be avoided. The minable percentage of the area is about 22%. In Fig. 20, craters less than

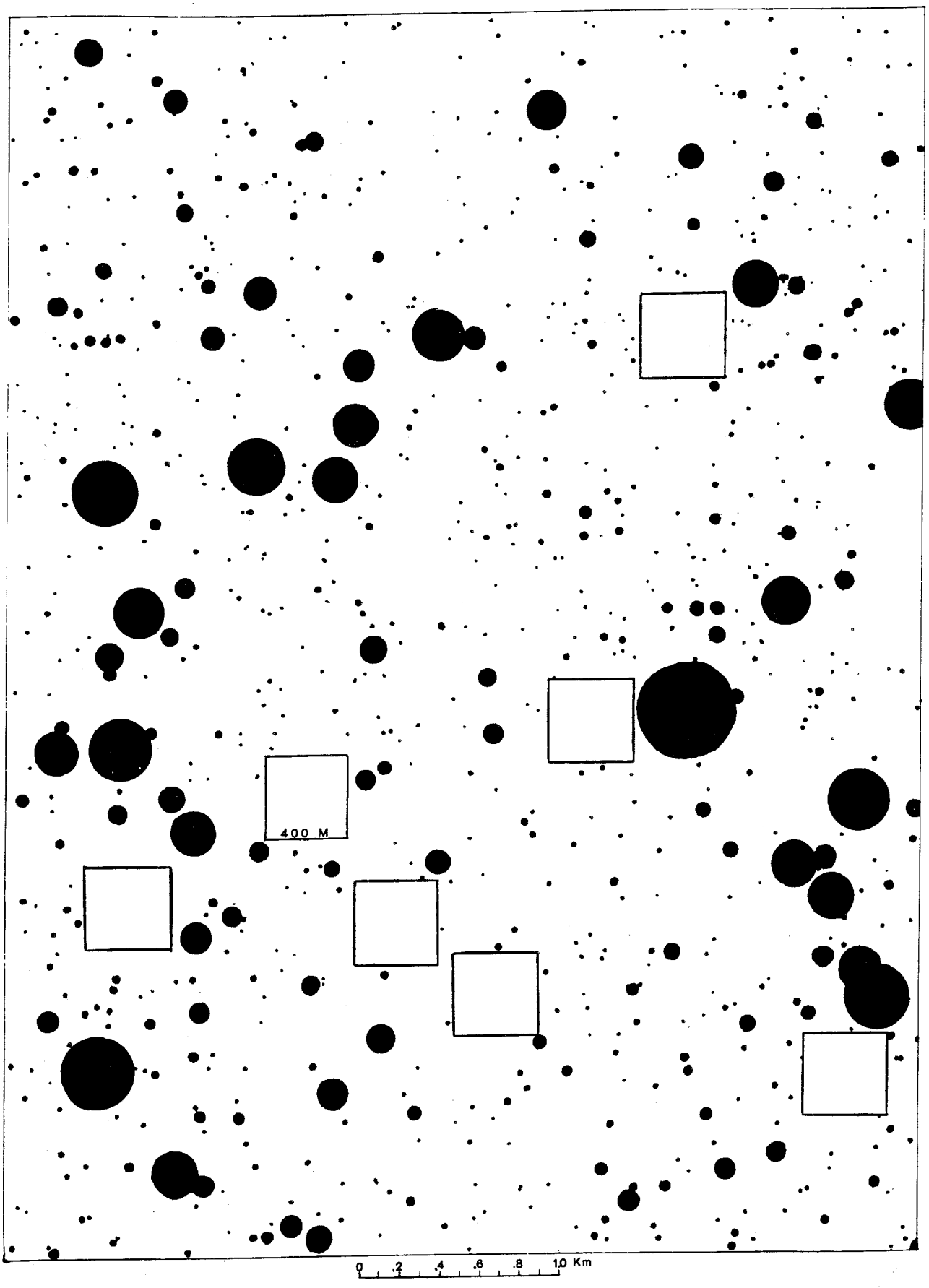

Fig. 17. Craters 11.7 m or more in diameter, with their inferred ejecta halos, plotted on an overlay of Fig. 16. Unit mining blocks are 400 m square.

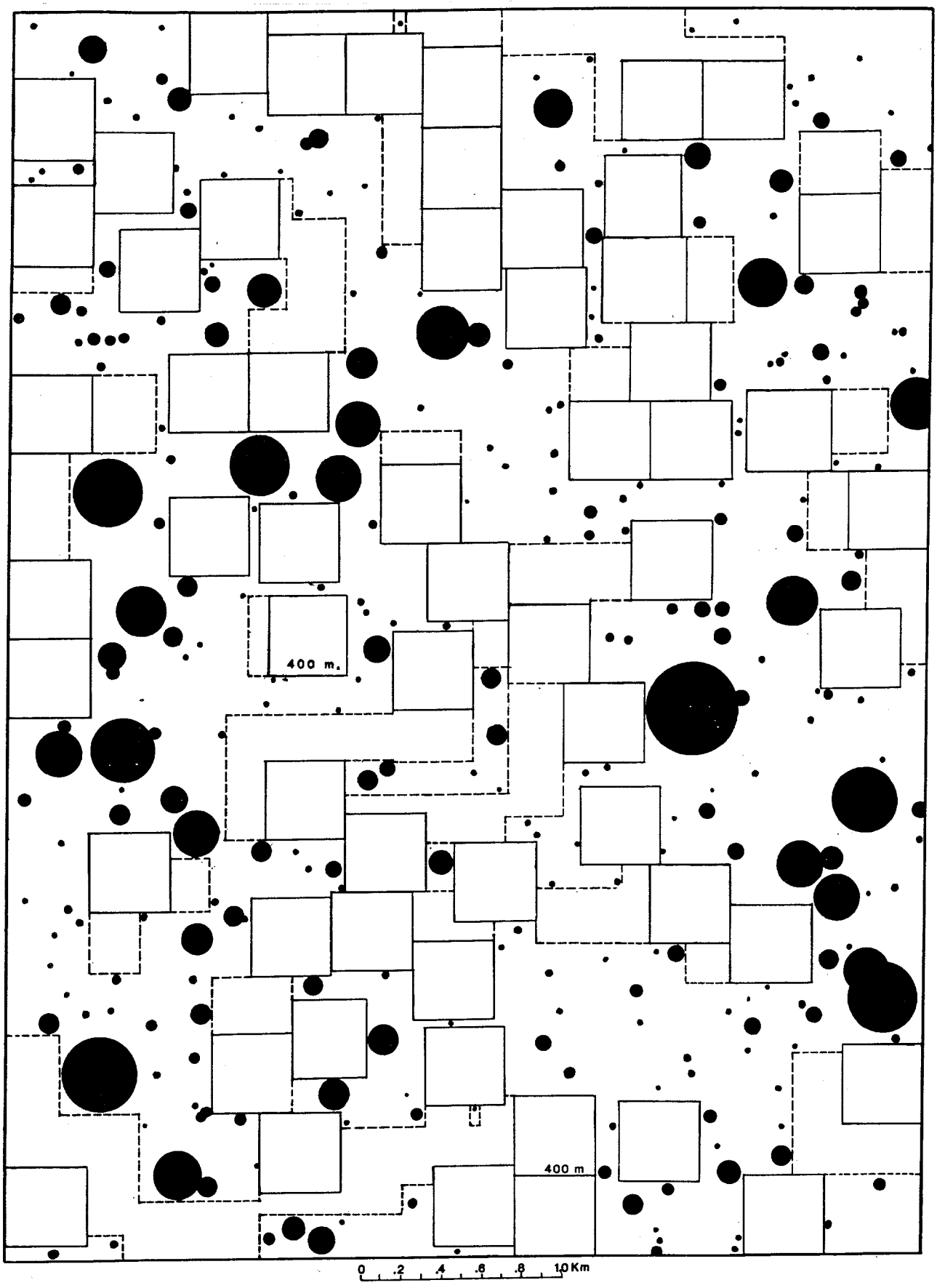

Fig. 18. Craters 23.4 m or more in diameter, with their inferred ejecta halos, plotted on an overlay of Fig. 16. Unit mining blocks are 400 m square; possible extensions are shown by dashed lines.

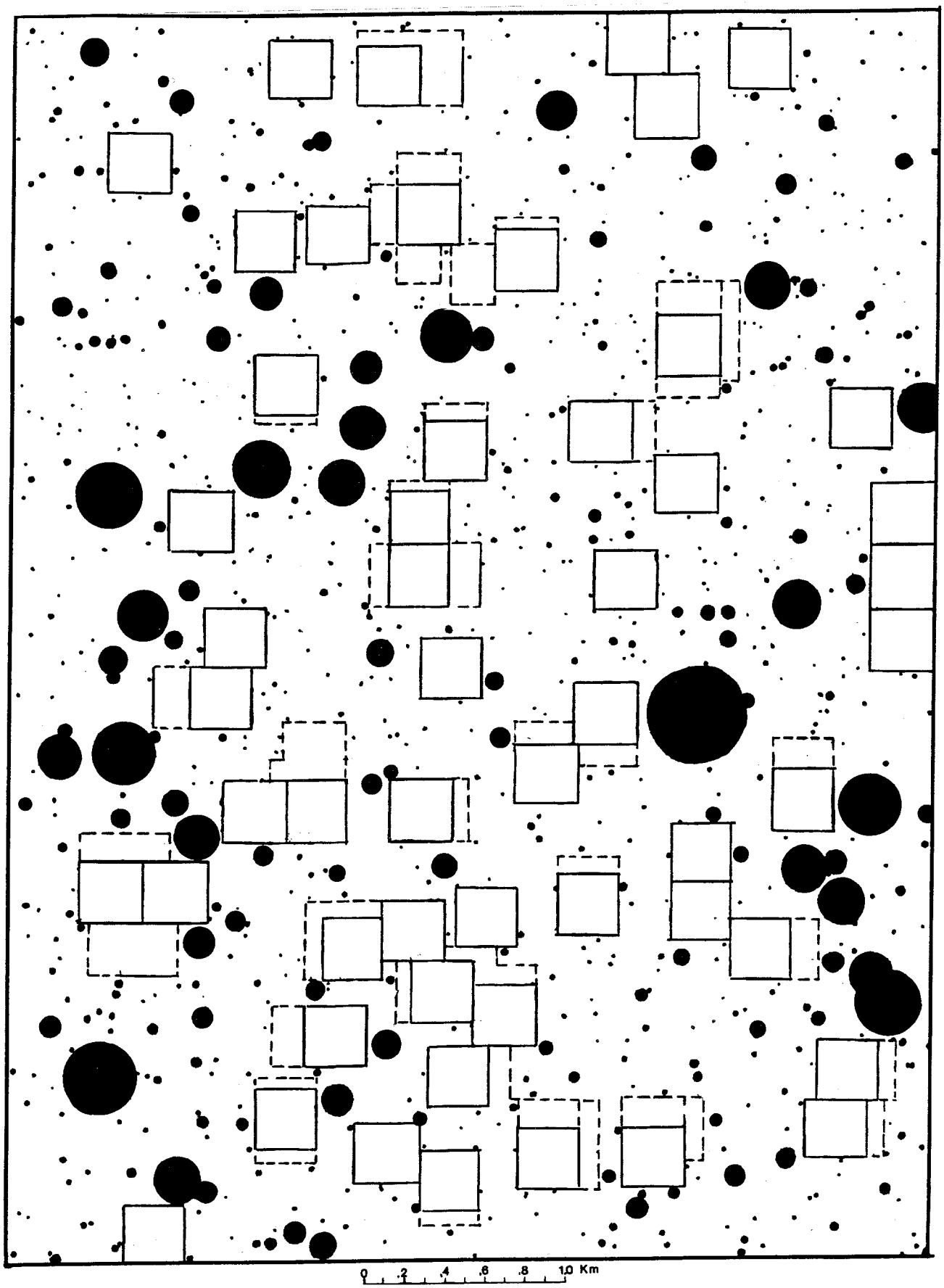

Fig. 19. Craters 11.7 m or more in diameter, with their inferred ejecta halos, plotted on an overlay of Fig. 16. Unit blocks are 300 m square; possible extensions are shown by dashed lines.

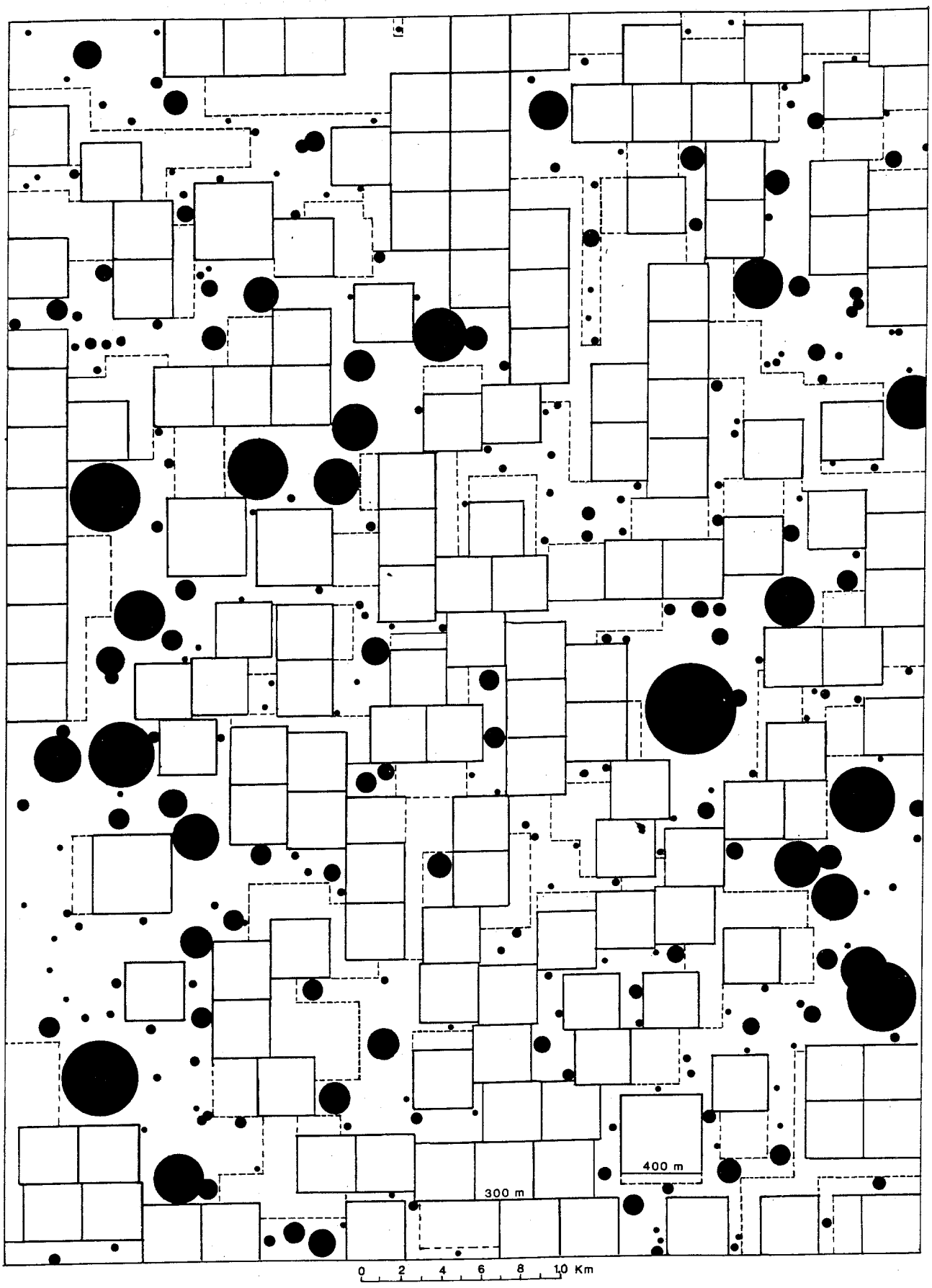

Fig. 20. Craters 23.4 m or more in diameter, with their inferred ejecta halos, plotted on an overlay of Fig. 16. Unit blocks are 300 m square; possible extensions are shown by dashed lines.

23.4 m in diameter can be mined. The minable percentage in unit blocks and sideward extensions is 56%, and the amount of regolith available is 95,200,000 tonnes.

Charts similar to those of Fig. 17 through 20 have been plotted for three additional prints for which the calculated percentages unminable due to craters and halos are 12.1 (II-88H2), 15.2 (II-86-H2), and 22.1% (II-83H2). The effect of unit block size on percentage of total area minable is shown in Fig. 21. For the area covered by each print, minable percentage reaches its maximum when the unit block size becomes zero, at which point the unminable area is equal to the percentage of the total area occupied by craters and blocky ejecta halos. It is evident that for any given area, the design of the mining equipment, in particular its maneuverability, will strongly affect the minable percentage.

The study suggests that for the Apollo 11 area minable portions will range from about 17% to 42% if the basic mining unit is 400 m square, or from 28 to 57% if the basic mining unit is 300 m square.

Amount of Helium in Minable Regolith of Mare Tranquillitatis

The data developed in preceding sections of this report provide the basis for an estimate of tonnage and grade of the regolith of Mare Tranquillitatis and an estimate of the amounts of He and ^{3}He available in it. The area of the mare is estimated at roughly 300,000 km^2, of which it is estimated that as much as 50% may be minable with a suitable mining system. The average thickness of regolith is taken as 3 m, although a greater average thickness appears to be indicated. Of the total area of the mare it is inferred that 28% is covered by regolith that contains 30 to 45 wppm total He, 65% by regolith that contains 20 to 30 wppm total He, and 7% by regolith that contains less than 20 wppm total He. The third category is too low in He to be of interest at present. Areas and minable tonnages of regolith, He, and ^{3}He represented in the first two categories are given in Table 11. Assumptions are: (1) 50% minability, (2) regolith thickness 3 m, and He (total)/^{3}He = 2600.

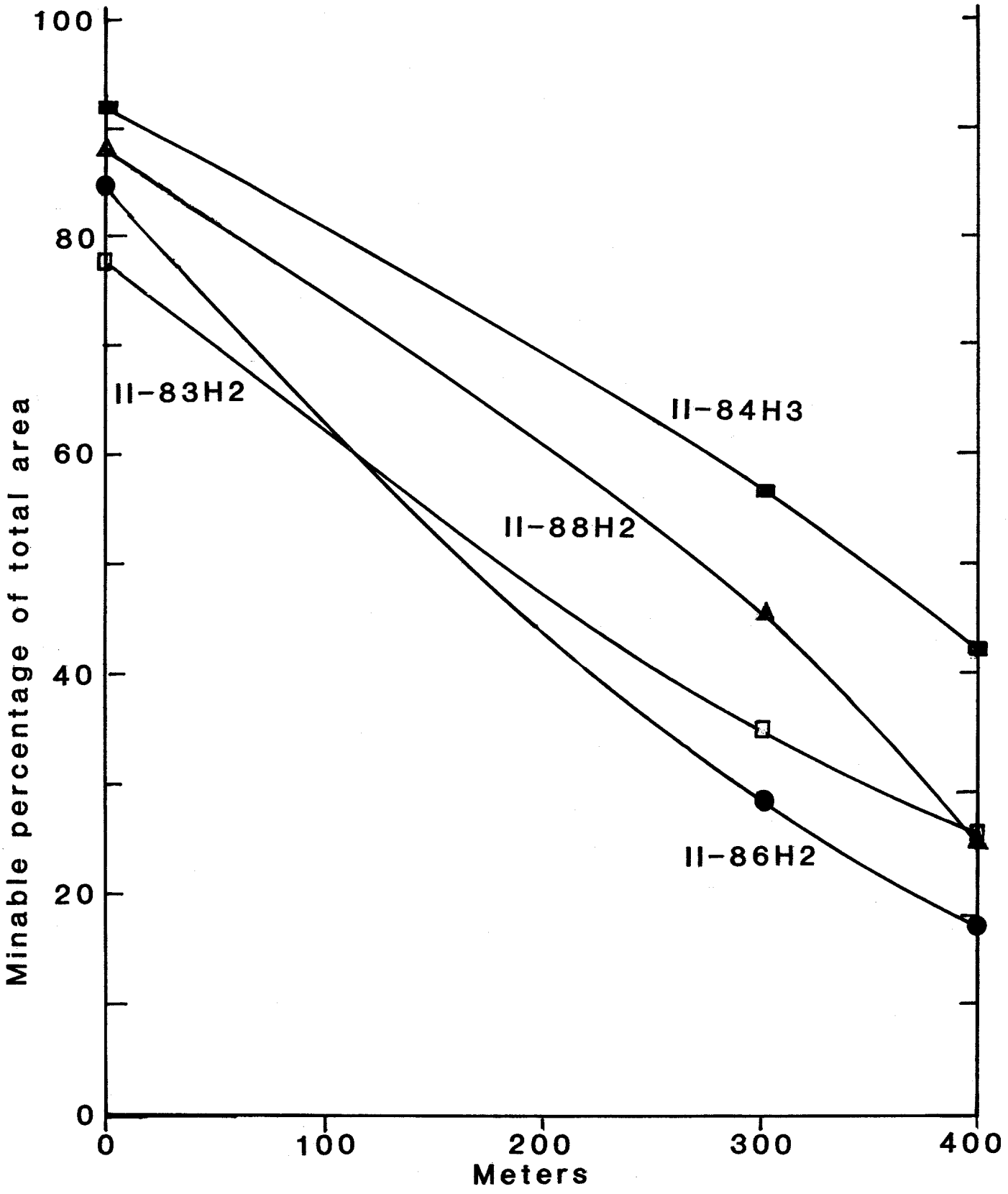

Fig. 21. Minable percentage of total area in relation to size of unit mining block.

Table 11

Minable Regolith and Helium Content of Mare Tranquillitatis

Regolith Category	Area in km^2	Average He Content wppm	Regolith Minable tonnes	He tonnes	^3He tonnes
A	84,000	38	252×10^9	9.58×10^6	3,635
B	195,000	25	598×10^9	14.96×10^6	5,754
Totals	279,000		850×10^9	24.54×10^6	9,439

Note: ^3He content based on $He/^3He = 2600$.

OTHER AREAS OF HIGH-TITANIUM REGOLITH

Remote sensing indicates that other areas of high-Ti regolith occur on the nearside of the Moon. Figure 22 shows the distribution of color groups of basaltic regolith indicated by spectral reflectance studies, with the inferred TiO_2 contents of each group. Substantial areas of high-TiO_2 regolith are indicated in Oceanus Procellarum, Mare Imbrium, Mare Humorum, and Mare Nubium, and smaller areas occur in Mare Insularum and southwest of Mare Serenitatis. The total of those areas is several times, perhaps 5 times, the total area of Tranquillitatis. No samples of regolith of those areas are yet available, but the areas certainly deserve investigation as possible sources of He. High-TiO_2 regolith with He in excess of 30 wppm was found by Apollo 17 in the Taurus-Littrow area, along the SE side of Mare Serenitatis; this appears to be a northern extension of the regolith of Tranquillitatis.

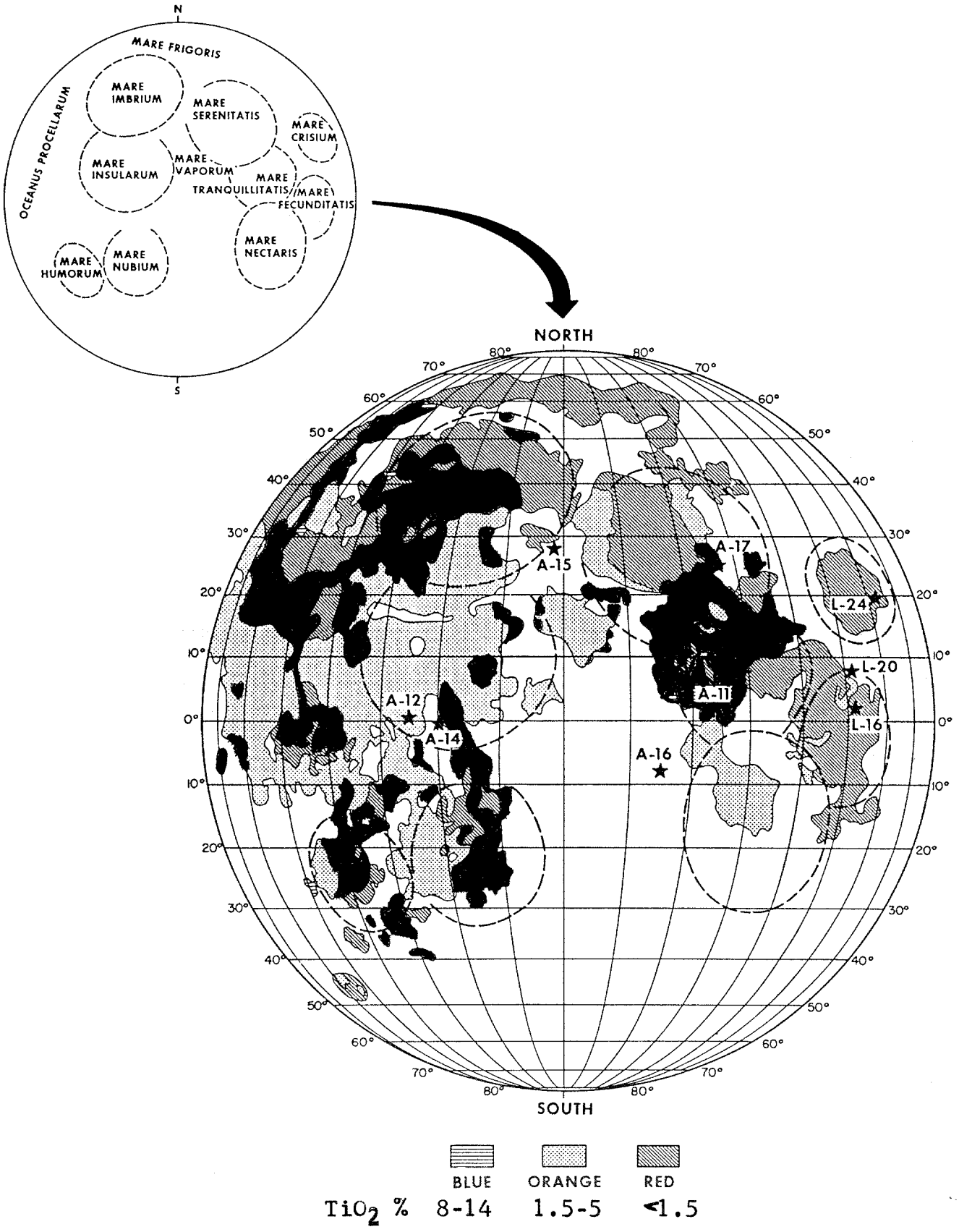

Fig. 22. Color groups of mare regoliths and the TiO_2 values thought to be represented by the groups. From Basaltic Volcanism Study Project, 1981, Lunar mare basalts. In Basaltic Volcanism on the Terrestrial Planets, Pergamon Press, pp. 236-267.

SUMMARY AND CONCLUSIONS

1) Mare Tranquillitatis occupies an area of about 300,000 km^2 on the near side of the Moon.

2) Major structural features, all unminable, are ridges, rilles, domes, islands of basement rocks, and major craters. They are most numerous in the western half of the mare. Ray materials are also present in parts of the mare, mostly in the western part. Their effect on minability is uncertain.

3) Regolith of Mare Tranquillitatis is derived predominantly from underlying basaltic volcanics but is diluted, to varying degrees, by ejecta composed of highland material.

4) Studies of very small craters indicate an average thickness of regolith of about 4.5 m.

5) The regolith consists predominantly of fine-grained (less than 100 μm) particles. Helium is mostly in the fine-grained material.

6) From part to part of the mare the average helium content of regolith, as inferred from sampling by Apollo 11 and from remote sensing, ranges from less than 20 wppm to at least 45 wppm. Both lateral and vertical small-scale variations are to be expected, but in any large portion of regolith these variations should average out and should not be of concern in mining regolith.

7) Decline in average He content of regolith with depth is not indicated by available data over a range of at least several meters and, given the nature of the impact gardening process, is not to be expected.

8) Information from remote sensing and sampling indicates that about 28% of the mare is occupied by regolith with 30-45 wppm He, about 65% by regolith with 20-30% wppm, and 7% by regolith with less than 20 wppm.

9) The percentage of a given area of the mare that is physically amenable to mining is determined fundamentally by the number, size and size distribution of medium-sized to small craters. However, the percentage will be strongly affected by the nature of the mining system, especially by its ability to handle ejecta blocks and by its maneuverability.

10) Assuming a capability for handling small ejecta blocks, and cost-efficient mining of unit blocks as small as 300 m square, measurements of craters and associated ejecta halos on high-resolution photographs indicate that from place to place the percentage of the mare physically minable will range from 28 to 57%. Minability of an average 40% seems assured. With design of mining machinery so as to permit mining of somewhat smaller unit areas, 50% minability should be achievable.

11) Assuming that the regolith averages 3 m in thickness and that 50% will be minable, Mare Tranquillitatis is estimated to contain 3,635 tonnes of ^{3}He in minable regolith containing 30-45 wppm total He, and 5,738 tonnes of ^{3}He in regolith with 20-30 wppm total He.

12) The western part of Mare Tranquillitatis, in which Ranger VIII and Apollo 11 landed, does not appear to be the most promising area for helium mining. Particularly in the southern part of this area, there are numerous prominent ridges and large patches of ray materials. In a belt near the western margin of the mare, there is a series of large craters, up to 45 km in diameter, and a group of volcanic domes up to about 20 km in diameter.

The 85,000-km^2 area of the northeastern part of the mare is much freer of major craters and ridges and appears much more amenable to mining than the western part of the mare. Remote sensing indicates that the regolith in this area is comparable in TiO_2 content, and presumably in helium content, to the regolith of the Apollo 11 area.

RECOMMENDATIONS

Verification of the helium potential of Mare Tranquillitatis should be a principal objective of the next lunar missions. The following are recommended as necessary steps toward verification:

A. 1) An orbital mission for high resolution photography of a strip along the 8° N. parallel from 28° E. to 40° E. This would give a photographic transect of the northeastern portion of the mare, outlined on Fig. 15, that is largely covered by high-TiO_2 regolith (see Fig. 14) and offers fewer major obstacles to mining than the remainder of the mare.

Ultimately, photographic coverage of the strip should be extended to the western boundary of the mare.

A gamma-ray scan of the northeastern part of the mare should be included in the initial mission, preferably with resolution far better than that of the earlier gamma-ray scans. The purpose would be to determine, in as much detail as possible, the distribution of high-Ti regolith.

2) Selection of a landing site in the vicinity of 8° N., 34° 20' E., as indicated on Fig. 23.

B. A manned lunar mission with the following capabilities:

1) a) Drilling regolith to depths of up to 5 m.

b) Core retrieval and sampling.

c) Ground radar, surveying to determine variations in depth of regolith and distribution of blocky ejecta.

d) Traversing, by lunar rover.

2) Drilling and sampling of regolith over whatever area is within reach of the rover, within the scope of the mission schedule. Radial traverses extending at least several kilometers from the landing site are desirable in order to check variations in TiO_2 and helium content suggested by the Whitaker photograph (Fig. 4) and by the gamma-ray scan recommended above. One extended traverse should run due east from the landing site, another due west from the site.

3) Acquisition of two 10-kg bulk samples of regolith, one for testing procedures for oxygen extraction from ilmenite, the other for testing procedures for separating fine size fractions prior to heating to release helium. Actually, this might be accomplished by a robotic mission.

4) Study of distribution of blocks in regolith, visually and by ground radar, relative to craters of various sizes and ages.

5) Study of craters of various ages with regard to physical minability.

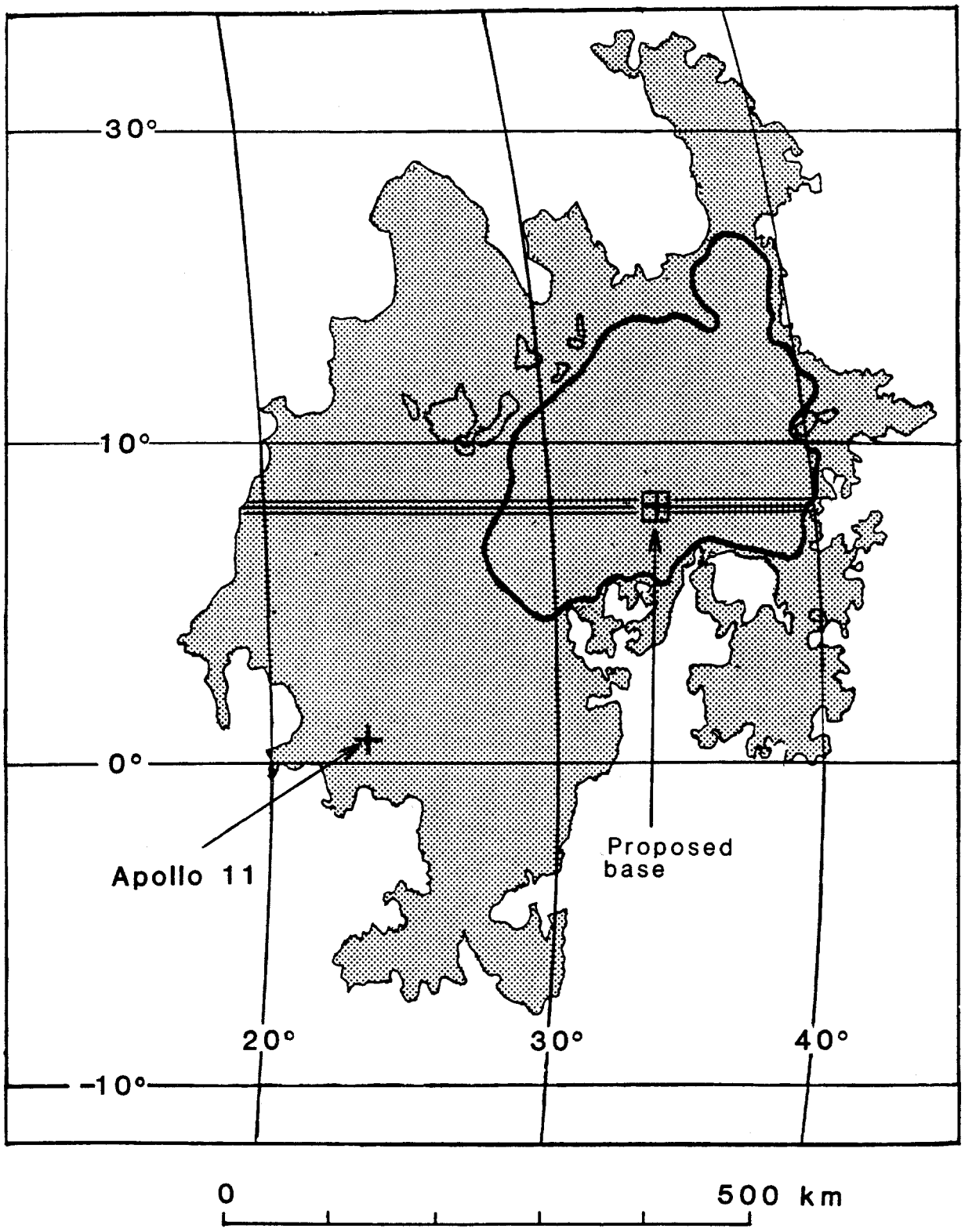

Fig. 23. Map of Mare Tranquillitatis showing proposed landing site for next lunar mission and transect (triple line) of the mare proposed for initial examination and systematic sampling.

ACKNOWLEDGMENTS

I am greatly indebted to Paul D. Spudis for his advice and for furnishing geologic maps of Mare Tranquillitatis and information on photographic coverage. I am also indebted to Harrison H. Schmitt for his thorough review and numerous helpful criticisms of the original draft of this report. Gerald L. Kulcinski and John F. Santarius have also contributed useful comments.

REFERENCES

Basaltic Volcanism Study Project, 1981, Lunar mare basalts. In Basaltic Volcanism on the Terrestrial Planets, Pergamon Press, pp. 236-267.

Bogard, D.D., and W.C. Hirsch, 1978b, Depositional and irradiational history and noble gas content of orange-black droplets in the 74001/2 core from Shorty Crater. Proc. 9th Lunar Sci. Conf., vol. 2, pp. 1981-2000.

Bogard, D.D., W.C. Hirsch, and L.E. Nyquist, 1974, Noble gases in Apollo 17 fines: mass fractionation effects in trapped Xe and Kr. Proc. 5th Lunar Sci. Conf., vol. 2, pp. 1975-2003.

Bogard, D.D., and L.E. Nyquist, 1972, Noble gas studies on regolith materials from Apollo 14 and 15. Proc. 3rd Lunar Sci. Conf., vol. 2, pp. 1797-1820.

Cameron, E.N., 1988, Titanium in lunar regoliths and its use in selecting helium-3 mining sites. Report WCSAR-TR-AR3-8708, Wisconsin Center for Space Automation and Robotics, Madison, WI, pp. 23.

Carr, M.H., 1965, Geologic map of the Mare Serenitatis quadrangle of the Moon. USGS Map I-489 (LAC 42), scale 1:1,000,000.

Criswell, D.R., and R.D. Waldron, 1982, Lunar utilization. In Space Utilization, B. O'Leary, ed., vol. II, CRC Press, Boca Raton, FL, pp. 1-53.

Cuttitta, H., H.J. Rose, Jr., C.S. Annell, M.K. Carron, R.P. Christian, E.J. Dwornik, L.P. Greenland, A.W. Helz, and D.T. Ligon, Jr., 1971, Elemental composition of some Apollo 12 lunar rocks and soils. Proc. Second Lunar Sci. Conf., vol. 2, pp. 1217-1229.

Cuttitta, F., Jr., H.J. Rose, Jr., C.S. Annell, M.K. Carron, R.P. Christian, D.T. Ligon, Jr., E.J. Dwornik, T.L. Wright, and L.P. Greenland, 1973, Chemistry of twenty-one igneous rocks and soils returned by the Apollo 15 mission. Proc. Fourth Lunar Sci. Conf., vol. 2, pp. 1081-1096.

David, P.A., 1980, Iron and titanium distribution in the Moon from orbital gamma-ray spectrometry with implications for crustal evolutionary models. J. Geophysics Res., vol. 85, pp. 3209-3224.

Eberhardt, P., J. Geiss, H. Graf, N. Grögler, U. Krahenbühl, H. Schwaller, J. Schwarzmuller, and A. Stettler, 1970, Trapped solar wind noble gases, exposure age and K/Ar age in Apollo 11 lunar fine material. Proc. Apollo 11 Lunar Sci. Conf., pp. 1037-1070.

Eberhardt, P., J. Geiss, H. Graf, N. Grögler, M.D. Mendia, M. Mörgeli, H. Schwaller, and A. Stettler, 1972, Trapped solar wind noble gases in Apolo 12 lunar fines 12002 and Apollo 11 breccia 10046. Proc. Third Lunar Sci. Conf., pp. 1821-1856.

Elston, D.P., 1972, Geologic map of the Colombo quadrangle of the Moon. USGS Map I-714 (LAC 79), scale 1:1,000,000.

Engster, O., P. Eberhardt, J. Geiss, N. Grogler, M. Jungck, and M. Morgeli, 1975, Solar-wind-trapped and cosmic-ray-produced noble gases in Luna 20 soil. Proc. 6th Lunar Sci. Conf., pp. 1989-2007.

Funkhouser, J., E. Jessberger, O. Muller, and J. Zahringer, 1970, Active and inert gases in Apollo 12 and Apollo 11 samples released by crushing at room temperature and by heating at low temperatures. Proc. 2nd Lunar Sci. Conf., vol. 2, pp. 1381-1396.

Grolier, M.J., 1970, Geologic map of the Sabine D region of the Moon, USGS Map I-618, scale 1:100,000.

Grolier, M.J., 1970, Geologic map of the Apollo site II (Apollo 11). USGS Map I-619, scale 1:1,000,000.

Haskin, L.A., P.A. Helmke, D.F. Blanchard, J.W. Jacobs, and K. Telander, 1973, Major and trace element abundances in samples from the lunar highlands. Proc. 4th Lunar Sci. Conf., vol. 2, pp. 1275-1296.

Heymann, D., J.L. Jordan, A. Walker, M. Dziczkaniec, J. Ray, and R. Palma, 1978, Inert gas measurements in the Apollo 16 drill core and an evaluation of the stratigraphy and depositional history of this core. Proc. Ninth Lunar Sci. Conf., vol. 2, pp. 1885-1912.

Heymann, D., and A. Yaniv, 1970, Inert gases in the fines from the Sea of Tranquillity. Proc. Apollo 11 Lunar Sci. Conf., vol. 2, pp. 1247-1259.

Heymann, D., A. Yaniv, and S. Lakatos, 1972, Inert gases in 12 particles and one dust sample from Luna 16. Earth Planet. Sci. Letters, vol. 13, pp. 400-406.

Heymann, D., A. Yaniv, and S. Lakatos, 1972, Inert gases from Apollo 12, 14, and 15 fines. Proc. 3rd Lunar Sci. Conf., vol. 2, pp. 1857-1863.

Hintenberger, H., H.W. Weber, H. Voshage, H. Wänke, F. Begemann, and F. Wlotzka, 1970, Concentrations and isotopic abundances of the rare gases, hydrogen, and nitrogen in lunar matter. Proc. Apollo 11 Lunar Sci. Conf., vol. 2, pp. 1269-1282.

Hintenberger, H., H.W. Weber, and N. Takaokoka, 1971, Concentration and isotopic abundances of rare gases in lunar matter. Proc. 2nd Lunar Sci. Conf., vol. 2, pp. 1617-1626.

Hintenberger, H., and H.W. Weber, 1973, Trapped rare gases in lunar fines and breccias. Proc. 4th Lunar Sci. Conf., pp. 2003-2020.

Hintenberger, H., H.W. Weber, and L. Schultz, 1974, Solar, spallogenic, and radiogenic rare gases on Apollo 17 soils and breccias. Proc. 5th Lunar Sci. Conf., vol. 2, pp. 2005-2022.

Hintenberger, H., L. Schultz, and H.W. Weber, 1975, A comparison of noble gases in lunar fines and soil breccias. Proc. 6th Lunar Sci. Conf., vol. 2, pp. 2261-2270.

Hübner, W., D. Heymann, and T. Kirsten, 1973, Inert gas stratigraphy of Apollo 15 core sections 15001 and 15003. Proc. 4th Lunar Sci. Conf., vol. 2, pp. 2021-2036.

Hübner, W., T. Kirsten, and J. Kiko, 1975, Rare gases in Apollo 17 soils with emphasis on analysis of size and mineral fractions of soil 74241. Proc. 6th Lunar Sci. Conf., vol. 2, pp. 2009-2026.

Johnson, T.V., R.S. Saunders, D.L. Matson, and J.L. Mosher, 1977, A TiO_2 abundance map for the northern maria. Proc. 8th Lunar Sci. Conf., vol. 1, pp. 1029-1036.

Kirsten, T., J. Deubner, P. Horn, I. Kaneoka, J. Kiko, O.A. Schaeffer, and S.K. Thio, 1972, The rare gas record of Apollo 14 and 15 samples. Proc. 3rd Lunar Sci. Conf., vol. 2, pp. 1865-1890.

Laul, J.C., and R.A. Schmitt, 1973, Chemical composition of Apollo 15, 16, and 17 samples. Proc. Fourth Lunar Sci. Conf., vol. 2, pp. 1349-1367.

Laul, J.C., and J.J. Papike, 1980, The lunar regolith: comparative chemistry of the Apollo sites. Proc. 12th Lunar Planet. Sci. Conf., vol. 2, pp. 1307-1340.

Ma, M.S., R.A. Schmitt, G.J. Taylor, R.D. Warner, D.E. Langer, and K. Keil, 1978, Chemistry and petrology of Luna 24 lithic fragments and -250 μm soils: Constraints on the origin of VLT basalts. In Mare Crisium: The View from Luna 24, Pergamon Press, New York, pp. 569-592.

Marti, K., G.W. Lugmair, and H.C. Urey, 1970, Solar wind gases, cosmic-ray spallation products and the irradiation history of Apollo 11 samples. Proc. Apollo 11 Lunar Sci. Conf., vol. 2, pp. 1357-1367.

Melosh, H.J., 1989, Cratering, A Geologic Process. Oxford University Press, New York, pp. 245.

Metzger, A.E., and R.E. Parker, 1980, The distribution of titanium on the lunar surface. Earth Planet. Sci. Letters, vol. 45, pp. 155-171.

Milton, D.J., 1968, Geologic map of the Theophilus quadrangle. USGS Map I-546 (LAC 78), scale 1:1,000,000.

Morris, E.C., and D.E. Wilhelms, 1967, Geologic map of the Julius Caesar quadrangle of the Moon. USGS Map I-510 (LAC 60), scale 1:1,000,000.

Nava, D.F., 1974, Chemical compositions of some soils and rocks from the Apollo 15, 16, and 17 lunar sites. Proc. 5th Lunar Sci. Conf., vol. 2, pp. 1087-1096.

Papike, J.J., S.B. Simon, and J.C. Laul, 1982, The lunar regolith: chemistry, mineralogy, and petrology. Geophysics and Space Physics, vol. 20, pp. 761-826.

Pepin, R.O., L.E. Nyquist, D. Phinney, and D.C. Black, 1970, Rare gases in Apollo 11 lunar material. Proc. Apollo 11 Lunar Sci. Conf., vol. 2, pp. 1435-1454.

Pieters, C., 1978, Mare basalt types on the front side of the moon: a summary of spectral reflectance data. Proc. 9th Lunar Planetary Sci. Conf., vol. 3, pp. 2825-2849.

Pieters, C., and T.B. McCord, 1976, Characterization of lunar mare basalt types: I. remote sensing study using reflectance spectroscopy of surface soils. Proc. 7th Lunar Sci. Conf., vol. 3, pp. 2677-2790.

Quaide, W.L., and V.R. Oberbeck, 1968, Thickness determinations of the lunar surface layer from lunar impact craters. J. Geophys. Res., vol. 73, pp. 5247-5270.

Quaide, W.L., and V.R. Overbeck, 1975, Development of the lunar regolith: Some model considerations. The Moon, vol. 13, pp. 227-551.

Rose, H.J., Jr., F. Cuttitta, S. Berman, F.W. Brown, M.K. Carron, R.P. Christian, E.J. Dwornik, and L.P. Greenland, 1974, Chemical composition of rocks and soils at Taurus-Littrow. Proc. 5th Lunar Sci. Conf., vol. 2, pp. 1119-1134.

Scott, D.H., and H.A. Pohn, 1972, Geologic map of the Macrobius quadrangle of the Moon. USGS Map I-789 (LAC 43), scale 1:1,000,000.

Shoemaker, E.M., R.M. Batsson, H.E. Holt, E.C. Morris, J.J. Renilson, and E.A. Whitaker, 1967, Television observations from Surveyor V. In Surveyor V, a preliminary report, NASA, pp. 9-42.

Shoemaker, E.M., and E.C. Morris, 1968, Jet Propulsion Laboratory, Surveyor Project Final Report, Part II, Science Results, pp. 86-136.

Shoemaker, E.M., M.H. Hait, G.A. Swann, D.L. Schleicher, G.G. Schaber, R.L. Sutton, D.H. Dahlem, E.N. Goddard, and A.C. Waters, 1970, Origin of the lunar regolith at Tranquility Base. Proc. Apollo 11 Lunar Sci. Conf., pp. 2399-2412.

Strom, R.G., 1972, Lunar mare ridges, rings, and volcanic complexes. In the Moon Symposium 47 of the International Astronomical Union, S. Runcorn and H. Urey, eds., Reidell, Dordrecht, pp. 187-215.

Sviatoslavsky, I.N., and M. Jacobs, 1988, Mobile helium-3 mining and extraction system and its benefits toward lunar base self-sufficiency. In Engineering, Construction, and Operations in Space, Proceedings of Space 88, E.W. Johnson and J.P. Wetzels, eds. Amer. Soc. of Civil Engineers, New York, pp. 310-321.

Wakita, H., and R.A. Schmitt, 1971, Bulk elemental composition of Apollo 12 samples: five igneous rocks and one breccia, and four soils. Proc. 2nd Lunar Sci. Conf., vol. 2, pp. 1231-1236.

Wänke, H., F. Wlotzksa, H. Baddenhausen, A. Balacescu, B. Spettel, F. Teschke, E. Jagouta, H. Kruse, M. Quijano, and R. Rieder, 1971, Chemical composition and its relation to sample locations and exposure ages, the two-component origin of the various soil samples, and studies on lunar metallic particles. Proc. 2nd Lunar Sci. Conf., vol. 2, pp. 1187-1208.

Whitaker, E.A., The surface of the moon. Chap. 3 of the Nature of the Moon (W.N. Ness, D.H. Menzel, and J.A. O'Keefe, eds.), Proc. 1965 International Astronomical Union Symposium, Baltimore, Johns Hopkins Press, pp. 79-98.

Wilhelms, D.E., 1972, Geologic map of the Taruntius quadrangle of the Moon. USGS Map I-722 (LAC 61), scale 1:1,000,000.

Wilhelms, D.E., 1987, The geological history of the Moon. U.S. Geol. Survey, Prof. Paper 1347, pp. 302.

Willis, J.P., A.J. Erlank, J.J. Gurney, H.H. Theil, and L.H. Ahrens, 1972, Major, minor, and trace element data for some Apollo 11, 12, 14, and 15 samples. Proc. Third Lunar Sci. Conf., pp. 1269-1273.